Fermilab Library
0 1160 0064838 0

— CLNS-97-1532 —

FERMILAB
DEC 22 1997
LIBRARY

CLNS 97/1532

Antiproton Sources

G. Dugan
Laboratory of Nuclear Studies
Cornell University
Ithaca, NY 14853
Cornell U, LNS

I. INTRODUCTION

Fig. 1 illustrates graphically the basic structure of an antiproton source[1,2,3,4], and lists its major technical issues. This description will emphasize these major issues, which are generally unique to antiproton sources. Many conventional accelerator physics issues, associated with the beam transport lines and the collection and accumulation rings, will not be discussed in detail in the interest of brevity.

In Fig. 1 and throughout this article, the Fermilab antiproton source[2,3] will be used as a specific example to illustrate the principles.

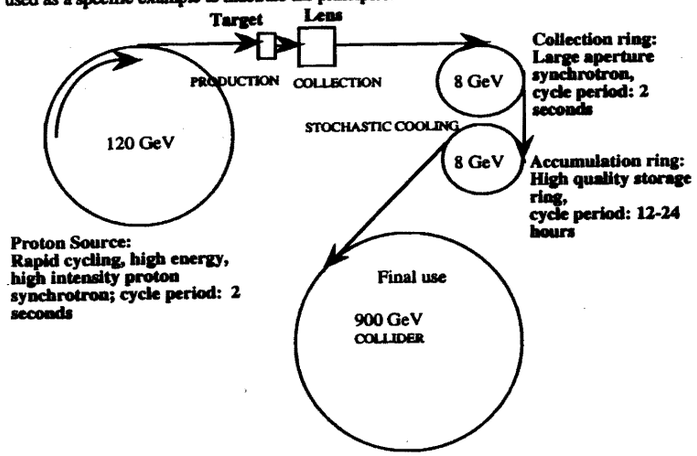

Major technical issues:

(1) antiproton production and collection

(2) antiproton beam density enhancement (through stochastic cooling).

Fig. 1 Basic components of an antiproton source (Fermilab energies)

II. ANTIPROTON PRODUCTION AND COLLECTION

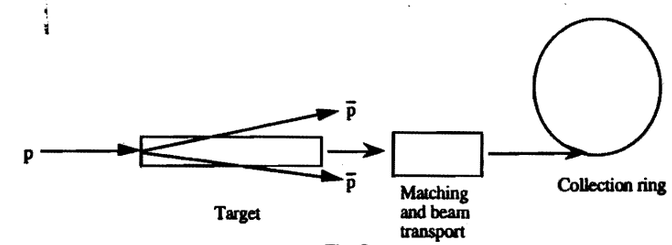

Fig. 2
The basic elements of the antiproton production/collection system

Fig. 2 shows schematically the principal elements of the antiproton production and collection system [5,6,7,8,9]. Antiproton production will be covered first.

A. Antiproton production

1. Transverse plane considerations

(a). Production cross section. Antiprotons are produced in high-energy p-nucleus collisions. The kinetic energy of the high-energy proton is converted to matter-antimatter pairs in the reaction

$$p + \text{nucleus} \rightarrow p + \text{nucleus}^* + (\bar{p} + p) + \text{other hadrons}$$

The production of antiprotons is conveniently described in terms of the differential yield,

$$\frac{\partial^2 Y}{\partial p \partial \Omega} = \frac{1}{\sigma_{abs}} \frac{\partial^2 \sigma}{\partial p \partial \Omega} \tag{2.1}$$

in which σ_{abs} is the proton absorption cross section in the target, and $\frac{\partial^2 \sigma}{\partial p \partial \Omega}$ is the differential antiproton production cross section. The forward yield rises with proton energy. For a given proton energy, the forward yield rises with antiproton energy to a peak or plateau [10,11,12].

(b). Antiproton phase space density: thin target approximation

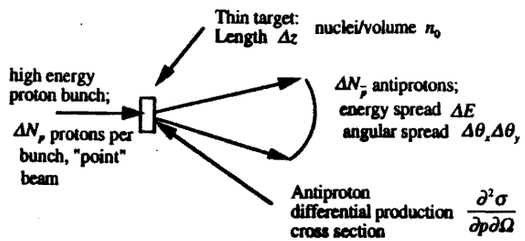

Fig. 3
Parameters used to describe the interaction of a proton bunch with a short target

Fig 3. defines some quantities involved in the interaction of a proton bunch with a very short target. The number of antiprotons produced per proton bunch on target is

$$\Delta N_{\bar{p}} = \Delta N_p \Delta z n_0 \left[\frac{\partial^2\sigma}{\partial p\partial\Omega}\Delta\theta_x\Delta\theta_y\Delta p\right] = \Delta N_p \frac{\Delta z}{\lambda}\left[\frac{\partial^2 Y}{\partial p\partial\Omega}\Delta\theta_x\Delta\theta_y\Delta p\right] \tag{2.2}$$

in which

$$\lambda = \frac{1}{n_0\sigma_{abs}} \tag{2.3}$$

is the proton absorption length in the target. For a proton beam with a finite extension, but with zero divergence at the target:

$$\Delta N_p = \rho\,\Delta x\,\Delta y, \tag{2.4}$$

where $\rho = \frac{\partial^2 N_p}{\partial x\partial y}$ is the proton density distribution in (x,y) space. The antiproton density distribution in phase space per unit momentum, per unit target length, is

$$\frac{\partial^2\bar{\rho}}{\partial p\partial z} = \frac{\partial^2}{\partial p\partial z}\frac{\partial^4 N_{\bar{p}}}{\partial x\partial\theta_x\partial y\partial\theta_y} = \frac{\rho}{\lambda}\frac{\partial^2 Y}{\partial p\partial\Omega} \tag{2.5}$$

For example, for a proton beam with a Gaussian transverse distribution

$$\rho(x,y) = \frac{N_p}{2\pi\sigma_x\sigma_y} Exp\left\{-\left(\frac{x^2}{2\sigma_x^2}+\frac{y^2}{2\sigma_y^2}\right)\right\} \tag{2.6}$$

with σ_x, (σ_y) the rms x(y) beam size on the target, and a differential yield whose angular dependence is also Gaussian (with rms width σ_θ),

$$\frac{\partial^2 Y}{\partial p\partial\Omega} = \frac{dY}{dp}\frac{1}{\pi\sigma_\theta^2} Exp\left\{-\left(\frac{\theta_x^2+\theta_y^2}{\sigma_\theta^2}\right)\right\} \tag{2.7}$$

the antiproton density is bi-Gaussian in x,y,θ_x, and θ_y:

$$\frac{\partial^2}{\partial p\partial z}\bar{\rho}(x,y,\theta_x,\theta_y) = \frac{dY}{dp}\frac{N_p}{2\lambda\sigma_x\sigma_y\pi^2\sigma_\theta^2} Exp\left\{-\left(\frac{\theta_x^2+\theta_y^2}{\sigma_\theta^2}+\frac{x^2}{2\sigma_x^2}+\frac{y^2}{2\sigma_y^2}\right)\right\} \tag{2.8}$$

The rms production angle $\sigma_\theta = p_t/p$ decreases roughly linearly as the antiproton energy increases, since p_t is roughly constant at a few hundred MeV (characteristic of the momentum transfer in hadronic processes).

Parameter	Approximate Value	Units	Symbol
Target parameters			
Proton absorption length in (tungsten) target	10	cm	$\lambda = \frac{1}{n_0\sigma_{abs}}$
Forward differential production yield	.118	$\bar{p}$/steradian/GeV/c/ proton	$\left.\frac{d^2Y}{dpd\Omega}\right\|_{\theta=0} = \frac{dY}{dp}\frac{1}{\pi\sigma_\theta^2}$
rms production angle	50	mrad	σ_θ
Target length	5	cm	L
Proton beam parameters			
Number of protons/bunch	2.5	10^{10}	N_p
Proton beam rms size in x,y on target	.04	cm	σ_x, σ_y
Proton beam bunch full time spread	.15	nsec	σ_t
Antiproton beam parameters			
Full energy spread of the collected antiproton beam at production	4% E=.36	GeV	ΔE
Full transverse emittance collected (both planes)	20	π mm-mrad	A_x, A_y
Antiproton mean velocity	.994	c	βk

Table I.
Example parameters related to antiproton production:(Fermilab antiproton source, original design [8])

For example, in Table I, the design parameters for the Fermilab antiproton source are given. Using these number, the forward antiproton transverse phase space density at production is roughly

$$\frac{\partial^2}{\partial p \partial z}\bar{\rho}(0,0,0,0) = \left[\frac{dY}{dp}\frac{1}{\pi\sigma_\theta^2}\right]\frac{N_p}{\lambda 2\pi\sigma_x\sigma_y}$$

$$= 0.118x10^{-4}\frac{2.5x10^{10}}{10x2\pi(0.4)^2} \approx 300 \ \frac{antiprotons}{(mm-mrad)^2(Gev/c)cm}$$

(c). Antiproton phase space density: thick target We allow the target to have a finite thickness, and consider the total number of antiprotons produced, integrated over all transverse phase space. The interaction length in the target for protons is given in Eq. (2.3); for antiprotons,

$$\bar{\lambda} = \frac{1}{n_0\bar{\sigma}_{abs}} \tag{2.9}$$

in which $\bar{\sigma}_{abs}$ is the antiproton total absorption cross section in the target. The total number of antiprotons per unit momentum produced from a target of length L is then

$$\frac{dN_{\bar{p}}}{dp} = \frac{exp(-\zeta)[1-exp(wL)]}{w\lambda}\frac{dY}{dp}N_p \tag{2.10}$$

in which $w = \frac{1}{\bar{\lambda}} - \frac{1}{\lambda}$ and $\zeta = \frac{L}{\lambda}$. For the case $\bar{\lambda} = \lambda$,

$$\frac{dN_{\bar{p}}}{dp}(\zeta) = \frac{dY}{dp}N_p\,\zeta exp(-\zeta) \tag{2.11}$$

This maximizes at $\zeta = 1$, or $L = \lambda$: a one interaction length target. From Table I, for the Fermilab design, we have for the total ratio of antiprotons produced per proton

$$\frac{1}{N_p}\frac{dN_{\bar{p}}}{dp}(\zeta) = \pi\sigma_\theta^2\left.\frac{d^2Y}{dpd\Omega}\right|_{\theta=0}\zeta exp(-\zeta)$$

$$= \pi(.050)^2(.118)(0.5)exp(-0.5) = 2.8x10^{-4}\ \frac{antiprotons}{proton\ (Gev/c)}$$

For the Fermilab design, the accepted momentum bite is about 0.36 GeV/c, and the collection efficiency is about 10 percent, leading to collected antiproton-to-proton ratios of about 10^{-5}.

The antiproton phase space density will depend on the transverse size of the incident proton beam, the length of the target, and the angular distribution of the antiproton differential yield. To illustrate the latter two dependencies qualitatively, consider Fig. 4 to 7.

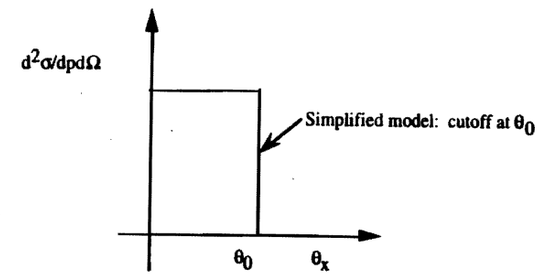

Fig. 4
Sharp-cutoff model for antiproton production cross section dependence on θ_x

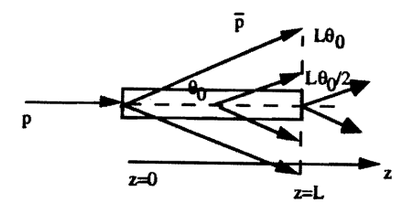

Fig. 5
Rays from three points in the target, in physical space

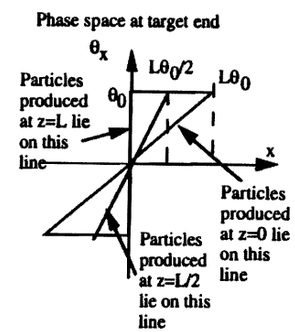

Fig. 6
Rays from Fig. 5, in transverse (x) phase space

Phase space at target center

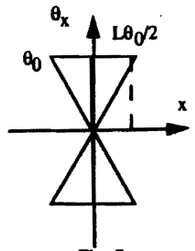

Fig. 7
Transverse phase space of Fig. 6, projected to target center

From the figures, it is seen that a finite length L target causes an effective source size for the antiprotons of order $L\sigma_\theta/2$. Because of the shape of Fig. 7, this is sometimes referred to as the "butterfly" effect. The finite size of the incident proton beam will result in an additional effective source size of order σ_x (at small θ_x). Typically, $\sigma_x << L\sigma_\theta/2$. For example, from Table I, $L\sigma_\theta/2$ =50x0.5/2 mm = 1.25 mm, but σ_x = 0.4 mm. The dominant contribution to the effective antiproton source size is that due to the finite target length.

An exact result for the antiproton phase space density from a thick target results from a solution to the transport equation. This equation (neglecting multiple Coulomb scattering in the target) is

$$\frac{\partial\bar{\rho}}{\partial z}+\vec{\theta}\bullet\vec{\nabla}\bar{\rho}+\frac{\bar{\rho}}{\lambda}=\frac{\rho}{\lambda}\frac{d^2Y}{dpd\Omega} \tag{2.12}$$

For a proton transverse density (round beam: $\sigma_x=\sigma_y=\frac{\sigma_r}{\sqrt{2}}$)

$$\rho(x,y,z)=\frac{N_p}{\pi\sigma_r^2}Exp\left\{-\left(\frac{x^2+y^2}{\sigma_r^2}\right)\right\}Exp\left[-\frac{z}{\lambda}\right] \tag{2.13}$$

and a Gaussian antiproton differential yield as given in Eq.. (2.7), the antiproton transverse phase space density from a target of length L, projected back to the center of the target, is

$$\frac{d}{dp}\bar{\rho}(x,\theta_x,y,\theta_y)=\frac{dY}{dp}\frac{N_p}{2\lambda\sqrt{\pi^3}\sigma_r\sigma_\theta^2\sqrt{\theta_x^2+\theta_y^2}}Exp\left\{-\left(\frac{\theta_x^2+\theta_y^2}{\sigma_\theta^2}\right)+a_1(x,\theta_x,y,\theta_y,L)-\frac{L}{\lambda}\right\}$$
$$\left[Erf\left(a_3(x,\theta_x,y,\theta_y,L)\right)-Erf\left(a_2(x,\theta_x,y,\theta_y,L)\right)\right] \tag{2.14}$$

in which

$$a_1(x,\theta_x,y,\theta_y,z)=\frac{1}{\theta_x^2+\theta_y^2}\left[\frac{(w\sigma_r)^2}{4}-w(x\theta_x+y\theta_y)-\frac{wz}{2}(\theta_x^2+\theta_y^2)-\frac{(x\theta_y-y\theta_x)^2}{\sigma_r^2}\right] \tag{2.15}$$

$$a_2(x,\theta_x,y,\theta_y,z)=\frac{1}{\sqrt{\theta_x^2+\theta_y^2}}\left[\frac{w\sigma_r}{2}-\frac{x\theta_x+y\theta_y}{\sigma_r}+\frac{z}{2\sigma_r}(\theta_x^2+\theta_y^2)\right] \tag{2.16}$$

$$a_3(x,\theta_x,y,\theta_y,z)=\frac{1}{\sqrt{\theta_x^2+\theta_y^2}}\left[\frac{w\sigma_r}{2}-\frac{x\theta_x+y\theta_y}{\sigma_r}-\frac{z}{2\sigma_r}(\theta_x^2+\theta_y^2)\right] \tag{2.17}$$

The density in (x, θ_x) phase space is

$$\bar{\rho}(x,\theta_x)=\int_{-\infty}^{\infty}d\theta_y\int_{-\infty}^{\infty}dy\bar{\rho}(x,\theta_x,y,\theta_y) \tag{2.18}$$

The result is

$$\frac{d}{dp}\bar{\rho}(x,\theta_x)=\frac{dY}{dp}\frac{N_p}{2\lambda\sqrt{\pi}\sigma_\theta\theta_x}Exp\left\{-\left(\frac{\theta_x^2}{\sigma_\theta^2}\right)+\frac{1}{\theta_x^2}\left[\frac{(w\sigma_r)^2}{4}-wx\theta_x-\frac{wL}{2}\theta_x^2\right]-\frac{L}{\lambda}\right\}$$
$$\left[Erf\left[\frac{w\sigma_r}{2\theta_x}-\frac{x}{\sigma_r}-\frac{L\theta_x}{2\sigma_r}\right]-Erf\left[\frac{w\sigma_r}{2\theta_x}-\frac{x}{\sigma_r}+\frac{L\theta_x}{2\sigma_r}\right]\right] \tag{2.19}$$

This is contour-plotted in Fig. 8, for the parameters given in Table I.

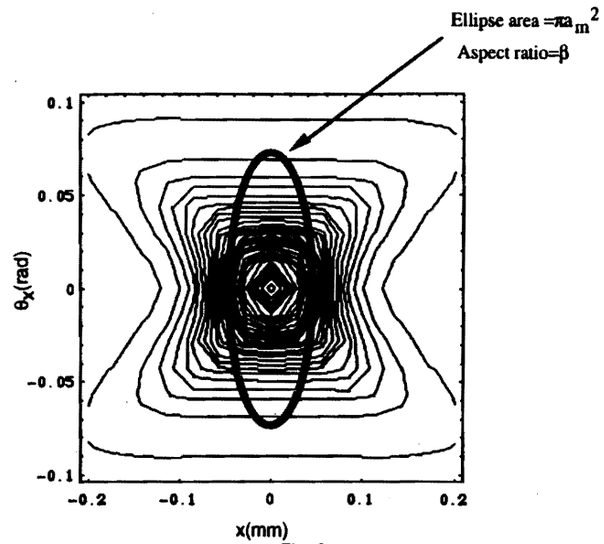

Fig. 8
Contours of constant antiproton phase space density for the example of Table I.

The density is modified mostly at small x due to the finite size of the proton beam, and falls off at large theta due to the Gaussian dependence of cross section on angle. The bulk of the density lies within the area $\pi\sigma_x\sigma_\theta$. The central density, for $\bar{\lambda}=\lambda$, is

$$\frac{d}{dp}\bar{\rho}(0,0,0,0,\zeta)=\frac{dY}{dp}\frac{N_p\zeta\, exp(-\zeta)}{\pi^2\sigma_\theta^2\sigma_r^2} \tag{2.20}$$

The number of antiprotons per unit momentum per bunch collected into the collection ring is then

$$\frac{dN_{\bar{p}}}{dp}=\int_{A_x,A_y}\frac{d}{dp}\bar{\rho}(x,y,\theta_x,\theta_y)dA_x dA_y \tag{2.21}$$

in which A_x, A_y are the areas in x,θ_x,y,θ_y phase space which the transport system and collection ring can accept (the transverse acceptance). For useful design estimates, the equations given above may be used to perform numerical integrations over the accepted regions of transverse phase space. Often the most useful technique is to use the density distributions as a sampling basis in a Monte Carlo ray tracing calculation through a transport line and collection ring with complicated aperture limits.

For simple numerical estimates of the yield, an analytical result can be obtained with some simplifying assumptions. We may transform the phase space variables into phase-

amplitude form, and do the integration over the phase variables in both planes. For upright acceptance ellipses at the target center with aspect ratios β_x,β_y the phase space density as a function of amplitude is

$$\frac{d}{dp}\bar{\rho}(a_x,a_y)=8N_p\frac{dY}{dp}\frac{Exp[-\frac{L}{\lambda}]}{\lambda\sigma_r^2\sigma_\theta^2}$$
$$\int_0^{\frac{L}{2}}d\eta\left\{\begin{array}{l}Exp\left[-\left(\frac{a_x^2\beta_x f_x(\eta)}{2\sigma_r^2}\right)\right]I_0\left[\frac{a_x^2\beta_x}{2\sigma_r^2}\sqrt{f_x(\eta)^2-\frac{4\sigma_r^2}{\beta_x^2\sigma_\theta^2}}\right]\\ Exp\left[-\left(\frac{a_y^2\beta_y f_y(\eta)}{2\sigma_r^2}\right)\right]I_0\left[\frac{a_y^2\beta_y}{2\sigma_r^2}\sqrt{f_y(\eta)^2-\frac{4\sigma_r^2}{\beta_y^2\sigma_\theta^2}}\right]\end{array}\right\} \tag{2.22}$$

in which

$$f_{x,y}(\eta)=1+\frac{\eta^2+\frac{\sigma_r^2}{\sigma_\theta^2}}{\beta_{x,y}^2} \tag{2.23}$$

and the amplitude variable a_x is related to x and θ_x by

$$a_x^2=\frac{x^2}{\beta_x}+\beta_x\theta_x^2 \tag{2.24}$$

with similar equations for y. The yield may be obtained by integrating up to the maximum accepted amplitude for each plane. If both planes have the same maximum "acceptance" a_m and the same β function at the target (see Fig. 8), then the result of this integration gives for the yield

$$\frac{dN_{\bar{p}}}{dp}=N_p\frac{dY}{dp}\zeta\, exp(-\zeta)\left[1-H(r,s,\frac{L}{\beta_0})\right] \tag{2.25}$$

where

$$H(r,s,x)=\frac{2}{x}\int_0^x dq\, Exp\left[-\frac{s^2g(q)}{2r}\right]\left[\begin{array}{l}Cosh\left(\frac{s^2}{2r}\sqrt{g(q)^2-4r^2}\right)\\ +\frac{g(q)}{\sqrt{g(q)^2-4r^2}}Sinh\left(\frac{s^2}{2r}\sqrt{g(q)^2-4r^2}\right)\end{array}\right] \tag{2.26}$$

In this expression

$$s=\frac{a_m}{a_0} \tag{2.27}$$

where

$$a_0^2=\sigma_r\sigma_\theta \tag{2.28}$$

is the characteristic emittance of the source; and

$$r = \frac{\beta_0}{\beta}, \tag{2.29}$$

where

$$\beta_0 = \frac{\sigma_r}{\sigma_\theta}, \tag{2.30}$$

is the characteristic aspect ratio of the source, and

$$g(q) = 1 + \frac{1}{r^2} + q^2 r^2 \tag{2.31}$$

For very large s, $H(r,s,\frac{L}{\beta_0})$ ->0, and we regain the formula for the total integrated yield. For finite s, the yield depends on the parameters s, r, and $\frac{L}{\beta_0}$. Fig. 9 below shows the dependence of the quantity $\left[1 - H(r,s,\frac{L}{\beta_0})\right]$ on the parameter s, for three values of r, and for a typical $\frac{L}{\beta_0}$=5 cm/7.5 mm.

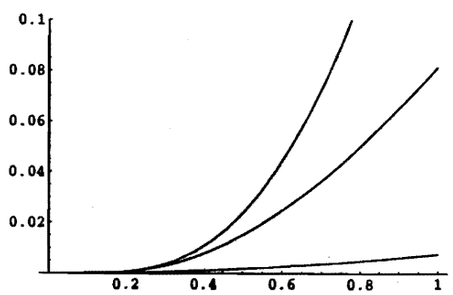

Fig. 9

$\left[1 - H(r,s,\frac{L}{\beta_0})\right]$ vs. s, for r=1.0,0.5, and 0.2. The upper curve is for r=1, and the lower for r=0.2.

For the Fermilab example, we have a_0^2 = 28 mm-mrad, and for the acceptances given in Table I, s is about .85, and $\left[1 - H(r,s,\frac{L}{\beta_0})\right]$ is about .12 for r=1. Fig. 9 illustrates the strong dependence of the yield on r: as β increases from the characteristic source aspect

ratio β_0 (about 7.5 mm for the Fermilab example), the yield is diminished rapidly. The collection lens (discussed below) is critical to achieving the optical match required to establish the proper value of $\beta \sim \beta_0$. The acceptance, which also determines the yield, is established by the apertures of the transfer line and collection ring.

The rate of antiproton production per unit momentum per second is

$$\frac{d\dot{N}_{\bar{p}}}{dp} = B\dot{C}\frac{dN_{\bar{p}}}{dp} \tag{2.32}$$

in which B= number of bunches per cycle of proton synchrotron and $\dot{C}$= number of cycles/second of the proton synchrotron. For the case of Fermilab, B=80 and $\dot{C}$=0.5 Hz, leading to

$$\frac{d\dot{N}_{\bar{p}}}{dp} = N_p B\dot{C}\frac{dY}{dp}\zeta Exp[-\zeta]\left[1 - H(r,s,\frac{L}{\beta_0})\right]$$

$$= 80x0.5x2.8x10^{-4}x0.12x2.5x10^{10}x3600\frac{antiprotons}{hr\ (Gev/c)} \approx 1.2x10^{11}\frac{antiprotons}{hr\ (Gev/c)}$$

(d). Target material limitations [13,14]. The energy deposited in the target per cycle by the proton beam, per unit mass of target, is

$$\frac{E_{deposited}}{m} = \left\{\frac{1}{\rho}\frac{dE}{dx}\right\}\frac{BN_p}{\pi\sigma_x\sigma_y} \tag{2.33}$$

From Eq. (2.22), the phase space density is proportional to $\frac{N_p}{\sigma_x\sigma_y}$; hence, to obtain more antiprotons, one wishes to maximize $\frac{E_{deposited}}{m}$. The energy deposited in the target causes the target's temperature to rise each cycle from T to T+ΔT, in which

$$\frac{E_{deposited}}{m} = \int_T^{T+\Delta T} c_p(T')dT' \tag{2.34}$$

where c_p is the specific heat of the target. If $\frac{E_{deposited}}{m}$ exceeds about 200-300 Joules/g, the rapid temperature rise may make the target susceptible to fracture due to thermal shock waves. Copper targets are often used, rather than tungsten, because, although their absorption length is longer, their ductility leads to a lack of extreme sensitivity to thermal shock, and so they can be operated at higher values of $\frac{E_{deposited}}{m}$ than tungsten.

This problem can be overcome to some extent through the use of a "beam sweeping" system [15], which scans the proton beam across the target during the beam pulse, to reduce the peak energy deposition. To avoid an increase of the effective source size, the collection optics must also be swept in synchronism.

2. Longitudinal plane considerations [16]

The duration of the antiproton proton pulse $\overline{\sigma}_t$ will be essentially the same as that of the protons σ_t. The longitudinal density of the antiprotons at production ,

$$\overline{\rho}_l \approx \frac{N_{\bar{p}}}{\sigma_t \Delta E} \tag{2.35}$$

will be maximized with a small value of σ_t. A bunch lengthening and rotation in longitudinal phase space in the proton synchrotron, just prior to extraction, is performed to reduce the value of σ_t for the beam delivered to the target.

The usual practice is first to adiabatically lengthen the beam on a flat top of the main synchrotron. This flat top lasts many synchrotron periods, and occurs just prior to extraction for antiproton production. The rf voltage is reduced adiabatically from $V_1 = V_{max}$ to $V_2 = V_{min}$. As a result, the bunch is lengthened and the energy spread is reduced. (Fig. 10)

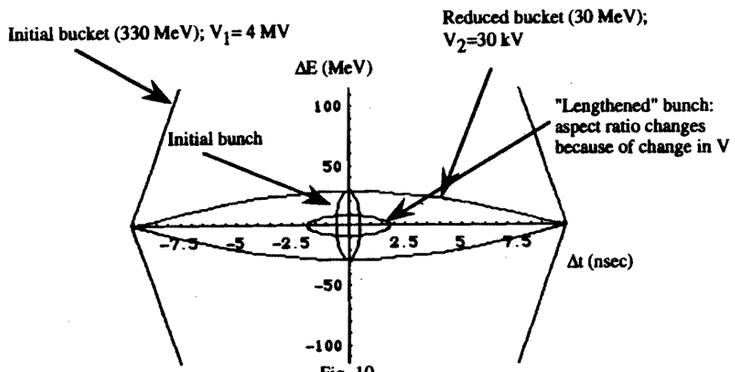

Fig. 10
Adiabatic bunch lengthening in the proton synchrotron
The numbers are exemplary of the Fermilab Antiproton Source

Then, the RF voltage is snapped rapidly back from V_2 to V_1, in a time very short compared to a synchrotron period (Fig. 11). The now-mismatched bunch rotates in the new bucket. If σ_{t0} was the original rms time spread of the proton bunch before the bunch lengthening, then the final time spread after the bunch rotation is

$$\sigma_t = \sigma_{t0}\left[\frac{V_2}{V_1}\right]^{\frac{1}{4}} \tag{2.36}$$

The beam is extracted at this point; the factor $\left[\frac{V_1}{V_2}\right]^{\frac{1}{4}}$ is typically in range of 3-4. The upper limit on V_1 is determined by the voltage capabilities of the proton synchrotron RF system; the lower limit on V_1 is limited by beam loading effects which become important at low voltages, and possibly also instability effects due to the small value of the momentum spread present just before the bunch rotation. Additional limitations arise from the natural non-linearities of the rf dynamics, which have been neglected above.
The beam transported to the target will have a momentum spread increased by the factor $\left[\frac{V_1}{V_2}\right]^{\frac{1}{4}}$, and the beam transport line from the proton synchrotron to the target , in particular the final focus to a small spot on the target, must have sufficient chromatic bandwidth to deal with this momentum spread.

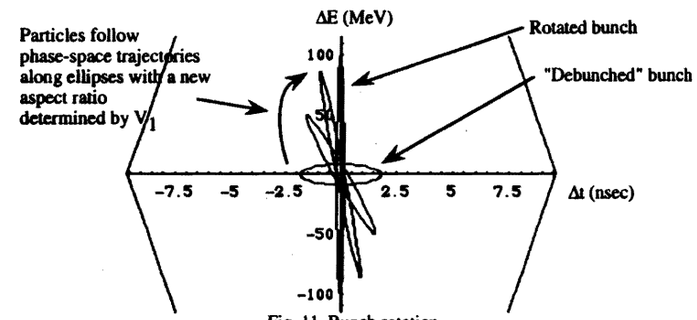

Fig. 11. Bunch rotation
The numbers are exemplary of the Fermilab Antiproton source.
The final time spread is σ_t=0.15 nsec.

B. Antiproton collection

1. Transverse plane considerations

The strongly divergent beam from the target must be focused into a parallel beam. Fig. 12 illustrates the mismatch problem.

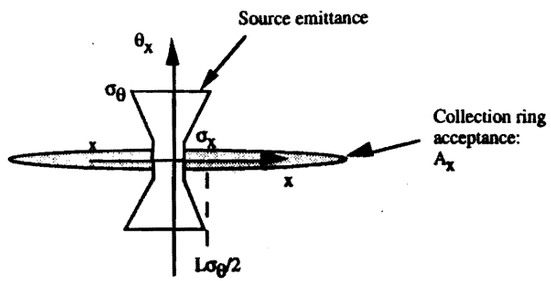

Fig. 12
Illustration of mismatch between source of antiprotons and typical acceptance of a collection ring.

The mismatch is corrected with a strong axisymmetric magnetic lens placed immediately after the target. (Fig. 13)

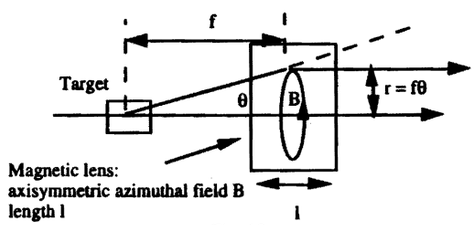

Fig. 13
Axisymmetric magnetic lens

The transverse kick delivered by the lens

$$p_t = e\int B dl \tag{2.37}$$

which gives a deflection angle:

$$\theta = \frac{p_t}{p} = \frac{e\int B dl}{p} \tag{2.38}$$

For axisymmetric point-to-parallel focusing, we require $\theta \propto r \Rightarrow B = Gr$, with G=lens gradient. In the thin lens approximation the lens focal length is

$$f = \frac{r}{\theta} = \frac{p}{e\int G dl} \approx \frac{p}{eGl} \tag{2.39}$$

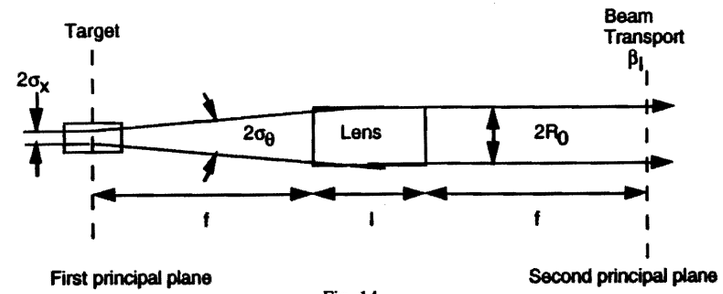

Fig. 14
Thick lens and target, showing focal length

For a lens of thickness l, the focal length (Fig. 14) is

$$f = \frac{1}{\sqrt{k}Tan(\mu)} \tag{2.40}$$

in which

$$k = \frac{eG}{p} \tag{2.41}$$

and

$$\mu = \sqrt{k}l \tag{2.42}$$

Fig. 15 shows the action of the linear lens in transverse phase space:

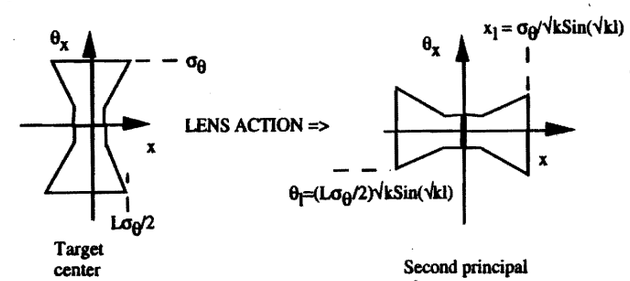

Fig. 15 Lens action in phase space

Referring to Fig. 15, from the requirement that $x_l \approx R_0$, we have that

$$R_0 \approx \frac{\sigma_\theta}{\sqrt{k}Sin(\sqrt{k}l)} \tag{2.43}$$

which sets the lens strength k to collect an angle σ_θ, for a given length l lens of radius R_0.

An additional requirement on the strength of the lens is related to the lattice function β_l, required for matching into the beam transport at the second principal plane of the lens. From Fig. 15,

$$\beta_l = \frac{x_1}{\theta_1} = \frac{2}{LkSin^2(\sqrt{k}l)} \tag{2.44}$$

If the beam transport optics determines β_l, Eq. (2.44) may be considered an additional condition on k which, together with Eq. (2.43), determines both k and R_0. Alternatively, if R_0 is fixed, for example, by lens engineering constraints, Eq. (2.44) may be considered to be a matching condition for the transport optics.

Axisymmetric focusing lenses which have been used include lithium lenses, horns and plasma lenses. In all cases, additional important considerations include minimizing antiproton absorption in the lens material (which is what motivates the use of lithium, the lowest density conductor), reducing multiple Coulomb scattering which will increase the emittance (again favoring low-Z materials), and obtaining reasonable good (1%) quadrupole field quality.

The transport line from the lens to the collection ring generally may be designed using standard beam line design practices. Matching of the optical functions is critical for high efficiency collection. The major unusual feature is the need for relatively high bandwidth (typical collection momentum spreads are in the range of 3%; see below). This may necessitate the use of sextupoles in dispersive regions of the transport line.

2. Longitudinal plane considerations [16]

The collection lens, transport system, and collection ring have a combined energy full width ΔE, which defines the momentum spread accepted from the target. However, the accumulation ring downstream from the collection ring generally must have a smaller momentum bandwidth for the injected beam. Hence it is necessary to reduce the momentum spread of the antiprotons in the collection ring. This may be done with a rotation by 90° in longitudinal phase space, followed by an adiabatic debunching.

The antiproton bunch from the production target will have the same time spread as that of the proton beam, called σ_t above.
This bunch is injected into the collection ring, in which the rf voltage is sufficiently large to accommodate the full energy spread ΔE from the target. The bunch is mismatched (see Fig 16) and rotates in the bucket.

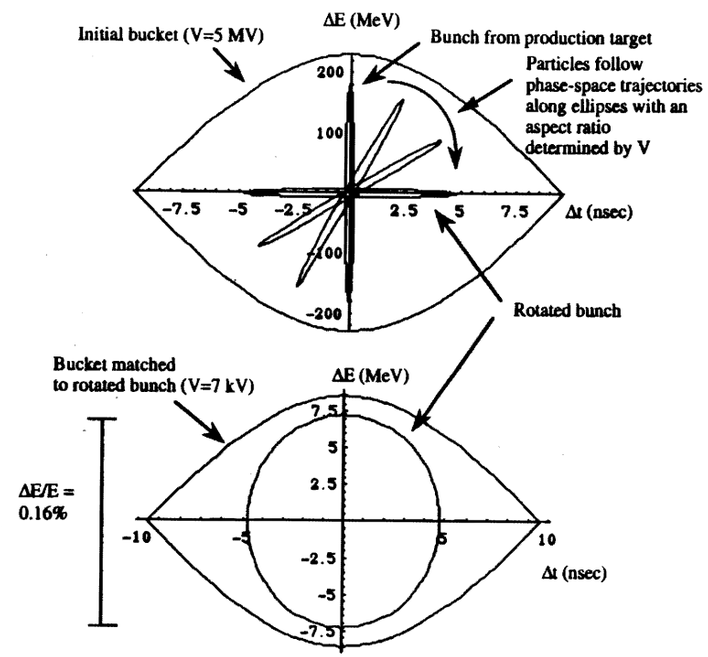

Fig. 16
Bunch rotation and adiabatic debunching in the collection ring.
This operation is performed on the antiprotons just after injection into the collection ring, and precedes any stochastic cooling.

Subsequently, as in Fig. 16, the rf voltage is reduced to zero and the beam is adiabatically debunched. If the entire process preserves the longitudinal emittance, then, we have, approximately

$$\sigma_t \Delta E \approx \frac{T_0}{2B} \Delta E_{fin} \tag{2.45}$$

in which B is the number of bunches injected into the collection ring, T_0 is the period of the collection ring, and ΔE_{fin} is the final full energy spread of the debunched beam. If

$$\Delta E_{fin} \approx \frac{2\sigma_t \Delta E B}{T_0} < (\Delta E)_a \tag{2.46}$$

in which $(\Delta E)_a$=the full momentum acceptance of the next (accumulation) ring, then the limit on the system momentum acceptance is the beam line/collection ring momentum aperture, ΔE, and the total number of antiprotons produced per cycle of the proton synchrotron is just

$$\frac{d\dot{N}_{\bar{p}}}{dC} \approx B\frac{dN_{\bar{p}}}{dp}\Delta E = B\Delta E N_p \frac{dY}{dp}\frac{l}{\lambda} Exp[-\frac{l}{\lambda}]\left[1 - H(r,s,\frac{l}{\beta_0})\right] \tag{2.47}$$

B is not really a free parameter, because the bunches must fit into the circumference of the collection ring, which requires

$$B < \frac{h^* T_0}{T_0^*} \tag{2.48}$$

in which h^* is the harmonic number, and T_0^* the period, of the proton synchrotron. Hence

$$\frac{d\dot{N}_{\bar{p}}}{dC} \approx h f_0 T_0^* \Delta E N_p \frac{dY}{dp}\frac{l}{\lambda} Exp[-\frac{l}{\lambda}]\left[1 - H(r,s,\frac{l}{\beta_0})\right] \tag{2.49}$$

In this case, the dependence on the details of the bunch length manipulations in the proton synchrotron and the collection ring do not appear.

If, on the other hand,

$$\Delta E_{fin} > (\Delta E)_a \tag{2.50}$$

then the limit on the system momentum acceptance is set by $(\Delta E)_a$, and the total number of antiprotons produced per cycle of the proton synchrotron is

$$\frac{d\dot{N}_{\bar{p}}}{dC} \approx \frac{dN_{\bar{p}}}{dp}(\Delta E)_a \frac{T_0}{2\sigma_t} = N_p \frac{dY}{dp}\frac{l}{\lambda} Exp[-\frac{l}{\lambda}]\left[1 - H(r,s,\frac{l}{\beta_0})\right](\Delta E)_a \frac{T_0}{2\sigma_t} \tag{2.51}$$

The production rate depends on the transverse parameters, on the time spread at extraction of the proton bunch in the proton synchrotron, on the efficiency of the longitudinal cooling, and on the energy aperture on the accumulation ring. This is generally not a good situation. In practice, if this is the case, one may employ fast longitudinal stochastic cooling(see below) to further reduce the momentum spread of the debunched antiproton beam prior to transfer to the accumulation ring, until ΔE_{fin} becomes less than $(\Delta E)_a$.

III. THE ANTIPROTON COLLECTION RING

Antiprotons from the target are injected into the collection ring. After the bunch manipulations described above, the debunched beam is cooled transversely (and longitudinally) to prepare for transfer into the limited acceptance of the accumulation ring.

A. Transverse Stochastic Cooling

1. Conceptual design: general results.

Fig. 17 illustrates the basic scheme [17,18,19,20,21,22,23,24,25,26].

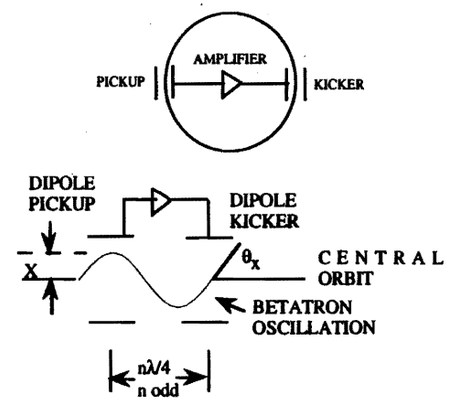

Fig. 17 Transverse stochastic cooling

The pickup measures the offset x from the reference trajectory of a sample of the beam; this signal is sent to a kicker, located an odd multiple of betatron quarter-wavelengths downstream. The kicker delivers a kick θ_x to the sample. This kick causes the position at the pickup on the next turn to be (x-gx), where g is called the "system gain". For such a system, in terms of g, the cooling rate for the transverse emittance ε is

$$\frac{1}{\tau_\varepsilon} = \frac{W}{N}\left[2g - g^2(M+U)\right] \tag{3.1}$$

in which W = system bandwidth, and N=number of particles in the ring. The "noise-to-signal" ratio is

$$U = \frac{6\pi\xi_{rms}^2 N}{WT\beta_{PU}\varepsilon} = U_0\frac{\varepsilon_0}{\varepsilon} \tag{3.2}$$

where U_0 is the value of U corresponding to the initial emittance ε_0. ξ_{rms}^2 is the rms system noise, measured as a position error at the pickup. T is the revolution period in the accumulation ring, and β_{PU} is the beta function at the pickup. The mixing factor M depends on the longitudinal beam density

$$M(\omega) = \frac{\pi f^2 \phi(\omega) ln 2}{W} \tag{3.3}$$

in which f=1/T is the revolution frequency, and the longitudinal density is

$$\phi(\omega) = \frac{1}{N}\frac{dN}{d\omega} \tag{3.4}$$

For a rectangular frequency distribution, with a full spread $\Delta\omega$ in the beam,

$$\phi(\omega) \approx \frac{1}{\Delta\omega} \tag{3.5}$$

and

$$M \approx \frac{f^2 \ln 2}{2W\Delta f} \tag{3.6}$$

Ideally, M = 1, but this is not always achievable in practice. If M>>1, the mixing is said to be "poor": it takes roughly M turns for the beam sample to become renewed. Cooling is only possible for $g \le \frac{2}{M+U}$; The cooling rate maximizes at the optimum value of g

$$g_{opt} = \frac{1}{M+U} \tag{3.7}$$

for which the cooling rate is

$$\frac{1}{\tau_c} = \frac{W}{N}\left[\frac{1}{M+U}\right] \tag{3.8}$$

With the appropriate value for g, cooling is always possible, no matter how large M and U are; however, the rate is inversely proportional to the sum of M and U. Note that the "noise-to-signal" ratio U (Eq. (3.2)) is a function of the emittance, and increases as the beam is cooled. The cooling rate, which depends on U, decreases, and there will be an asymptotic value of the final emittance to which the beam will finally cool. This is given by solving the following equation for the asymptotic emittance ε_∞:

$$\frac{d\varepsilon}{dt} = \frac{W}{N}\left(2g - g^2\left[M + U_0\frac{\varepsilon_0}{\varepsilon_\infty}\right]\right) = 0 \tag{3.9}$$

The result is

$$\frac{\varepsilon_\infty}{\varepsilon_0} = \frac{U_0}{2/g - M} = \frac{U_0}{M + 2U_0} \tag{3.10}$$

where the last result follows if we use $g = g_{opt}$. It is clear that we want M>>U_0 to achieve a small value for ε_∞. Some systems [27] have "plunging pickups" in which the system gain g is increased during the cooling cycle as the beam cools, to maintain close to the optimum gain at all times despite the increase in U.

2. *Single-particle cooling*

(a) Coherent cooling rate. Consider just one particle in the ring, undergoing a betatron oscillation with amplitude x at the pickup. The kicker delivers a kick angle θ_x to the particle, where the proportionality between x and θ_x, and the appropriate time synchronization, is provided by the stochastic cooling system. (Fig. 17) The devices used as pickups and kickers are usually stripline couplers [28,29], as shown in Fig. 18.

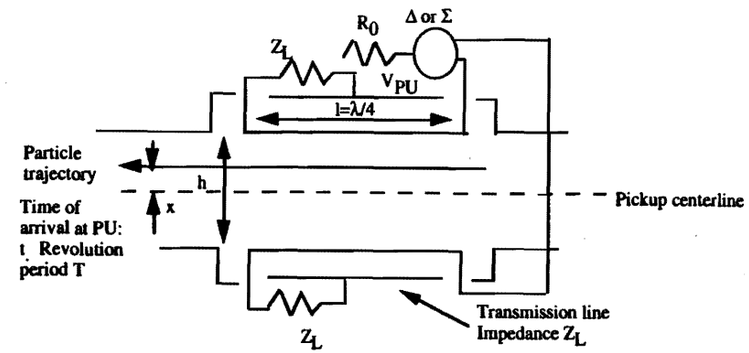

Fig. 18
Loop(stripline) coupler beam pickup (kicker)
length l, width w, gap h;
R_0 = output impedance (typically 50 Ω)
Z_L=characteristic impedance of the transmission line
l=λ/4, where f=c/λ is a frequency at the middle of the desired bandwidth.

For such a device, the voltage produced by the beam in the dipole pickup is determined by the (frequency dependent) transverse impedance $Z_\perp(\omega)$

$$Z_\perp(\omega) = \sqrt{\frac{R_0 Z_L}{2}}\frac{d(0,0)}{h} Sin[\theta(\omega)] Exp[i(\frac{\pi}{2} - \theta(\omega))] \tag{3.11}$$

in which $\theta(\omega) \approx \frac{\omega l}{c}$ and $d(0,0) = 2Tanh[\frac{\pi w}{2h}]$ is the on-axis transverse sensitivity. Summing over the harmonic structure (betatron sidebands) of the beam, the voltage from the pickup due to one particle is

$$V_{PU}(t) = \sqrt{\varepsilon\beta_{PU}}\frac{ef}{2}\sum_{n=-\infty}^{\infty}{}_{\pm} Z_\perp(\{n \pm Q\}\omega) Exp[i\{n \pm Q\}\omega t - in\omega t_{PU} \pm i\psi] \tag{3.12}$$

in which ε=emittance of the particle, β_{PU}=beta function at the pickup, $f = \frac{\omega}{2\pi}$=revolution frequency of the particle, t_{PU} = time of arrival of the particle at the pickup, Q=betatron tune of the particle, and ψ=betatron phase of the particle at the pickup.

Typically a number n_P of pickups is used, and the power is summed into a signal combiner:

$$P_{PU,\Sigma}(t) = n_P P_{PU}(t) \tag{3.13}$$

The total voltage is

$$V_{PU,\Sigma}(t) = \sqrt{n_P} V_{PU}(t) \tag{3.14}$$

This voltage is amplified (multiplied by $g_A(\omega)$, the amplifier gain function) and delivered to the kicker after a time delay of L/c, where L is the electrical length of the pickup-amplifier-kicker system. For a harmonically varying pickup voltage, the voltage to the kicker is

$$U_K(t) \propto g_A(\omega)V_{PU}(\omega)Exp(-i\omega(t-\frac{L}{c})) \tag{3.15}$$

The relationship between the voltage applied to the kicker $U_K(\omega)$, and the kick angle which the particle receives $\theta_x(t)$, is parameterized in terms of the kicker sensitivity $K_\perp(\omega)$:

$$\theta_x(t) \propto \frac{eU_K(\omega)K_\perp(\omega)}{\beta_k^2 E}Exp(-i\omega t) \tag{3.16}$$

for a harmonically varying kicker voltage $U(\omega)Exp(-i\omega t)$. Here β_k is the particle's velocity, and E its energy. The stripline kicker sensitivity is

$$K_\perp(\omega) = \sqrt{\frac{Z_k}{2R_0}}2d(0,0)\frac{c}{h\omega}Sin[\theta(\omega)]Exp[-i\theta(\omega)] \tag{3.17}$$

The total kicker voltage U_K is divided through power splitters to feed n_K kickers. Each kicker receives power

$$P_{K,n}(t) = \frac{P_K(t)}{n_K} \tag{3.18}$$

and thus voltage

$$U_{K,n}(t) = \frac{U_K(t)}{\sqrt{n_K}} \tag{3.19}$$

The total coherent kick is then

$$\theta_x(t) = \frac{e^2 f\sqrt{\varepsilon\beta_{PU}n_P n_K}}{2\beta_k^2 E}\sum_{\substack{n=-\infty \\ \pm}}^{\infty} F(\{n\pm Q\}\omega)Exp[i\{n\pm Q\}\omega(t-\frac{L}{c}) - in\omega t_{PU} \pm i\psi] \tag{3.20}$$

in which

$$F(\omega) = g_A(\omega)Z_\perp(\omega)K_\perp(\omega) \tag{3.21}$$

This kick is sampled by the particle as it passes through the kicker at time τ, at which its betatron phase is $\psi + \psi_{PK}$, where ψ_{PK} is the betatron phase advance from pickup to kicker. The emittance change from this kick must be averaged over many revolution periods, and also averaged over a random distribution in the initial betatron phase ψ at the pickup.

Finally, one requires timing synchronization between the pickup and kicker (Fig. 19).

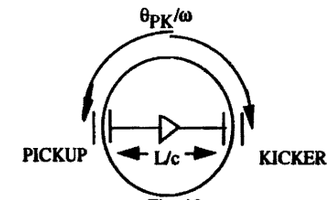

Fig. 19
Timing synchronization condition:
Electrical delay time (neglecting dispersion) = L/c
L=system electrical length

If θ_{PK} = azimuthal angular distance along the ring from pickup to kicker, then the timing synchronization condition is

$$(\tau - t_{PU}) = \frac{\theta_{PK}}{\omega} = \frac{L}{c} \tag{3.22}$$

Since the beam has a spread in frequency, this timing condition cannot be satisfied for all particles simultaneously. We choose to satisfy it for the mean frequency of the beam:

$$\theta_{PK} = \overline{\omega}\frac{L}{c} \tag{3.23}$$

Then $\Delta\omega = \omega - \overline{\omega}$ is the deviation of particle's frequency from the mean of the beam. The phase and time averaged emittance change produced by the cooling system, with this condition applied, is then

$$\langle\Delta\varepsilon\rangle = \frac{e^2 f\varepsilon\sqrt{\beta_{PU}\beta_K n_P n_K}}{2\beta_k^2 E}\sum_{\substack{n=-\infty \\ \pm}}^{\infty}(\mp i)F(\{n\pm Q\}\omega)Exp[\mp i\psi_{PK} - in\theta_{PK}\frac{\Delta\omega}{\overline{\omega}}] \tag{3.24}$$

From the average emittance change, the coherent ("single-particle") damping rate is

$$\frac{1}{\tau} = -\frac{\langle\Delta\varepsilon\rangle}{\varepsilon T} = \frac{e^2 f^2\sqrt{\beta_{PU}\beta_K n_P n_K}}{2\beta_k^2 E}\sum_{\substack{n=-\infty \\ \pm}}^{\infty}(\pm i)F(\{n\pm Q\}\omega)Exp[\mp i\psi_{PK} - in\frac{\Delta\omega}{\overline{\omega}}\theta_{PK}] \tag{3.25}$$

(b). Phase requirements . Suppose that $\Delta\omega = 0$. We want the real part of $(\pm i)F(\{n\pm Q\}\omega)Exp[\mp i\psi_{PK}]$ at each sideband to be positive to get damping. Take

$$F(\{n\pm Q\}\omega) = AExp[i\phi] \tag{3.26}$$

Then we want

$$Re(\pm iExp[\mp i\psi_{PK} + i\phi]) = \mp Sin[\mp\psi_{PK} + \phi] \tag{3.27}$$

to be positive, and optimally =1. This requires for the positive sideband (top sign):

$$\psi_{PK} - \phi = \frac{\pi}{2} + 2\pi m, \quad m=0,1,2,.. \tag{3.28}$$

for the negative sideband

$$\psi_{PK} + \phi = \frac{\pi}{2} + 2\pi n, \quad n=0,1,2... \tag{3.29}$$

These conditions can both be satisfied only if ϕ is an integer multiple of π: If ϕ = even multiple, $\psi_{PK}=\pi/2, 5\pi/2, 9\pi/2$, etc. If ϕ = odd multiple, $\psi_{PK}=3\pi/2, 7\pi/2, 11\pi/2$, etc.;

Now allow $\Delta\omega \neq 0$, and consider the term $Exp[-in\frac{\Delta\omega}{\overline{\omega}}\theta_{PK}]$: To obtain cooling at all harmonics, we require for all n within system bandwidth:

$$n\frac{\Delta\omega}{\overline{\omega}}\theta_{PK} < \frac{\pi}{2} \Rightarrow n < n_{max} = \frac{\overline{\omega}}{\Delta\omega}\frac{1}{4f_{PK}} \tag{3.30}$$

where f_{PK} is the fraction of the ring's azimuth between pickup and kicker. For $n > n_{max}$, we loose cooling. Because it corresponds in the time domain picture to particles leaving the sample between pickup and kicker, this effect is sometimes called "bad mixing".

(c). Simplifying assumptions. Let

$$\frac{e^2 fN\sqrt{\beta_{PU}\beta_K n_P n_K}}{\beta_k^2 E} F(\{n+Q\}\overline{\omega}) = h_n \tag{3.31}$$

(we neglect the very small variation of F over the beam frequency distribution) and take $\Delta\omega = 0$, $\psi_{PK} = \frac{\pi}{2} + 2\pi m$, to get

$$\frac{1}{\tau} = \frac{f}{N}\sum_{n=-\infty}^{\infty} h_n \tag{3.32}$$

If we convert the sum over harmonics to an integral

$$\sum_{n=-\infty}^{\infty} \rightarrow \frac{2}{f}\int_{f_1}^{f_2} df' \tag{3.33}$$

and extend this over the system bandwidth from $f_1 = W$ to $f_2 = 2W$, we have

$$\frac{1}{\tau} = \frac{2W}{N} h \tag{3.34}$$

in which h is the average of h_n over the system bandwidth:

$$h = \frac{\int_{f_1}^{f_2} df' h_n}{W} \tag{3.35}$$

Comparison with the equivalent coherent term in Eq.(3.1), in terms of the "system gain" g, allows the approximate identification:

$$g \approx h = \frac{e^2 fN\sqrt{\beta_{PU}\beta_K n_P n_K}}{\beta_k^2 E}\langle F(\{n+Q\}\overline{\omega})\rangle \tag{3.36}$$

where the average is meant to be taken over the system bandwidth.

(d). Example: Fermilab Debuncher 2-4 GHz transverse cooling system [30,31]. The pickup/kicker parameters are h=2.5 cm; w=2.25 cm; l=2.5 cm; W=2 GHz; Z_L= 83Ω (see Fig. 20)

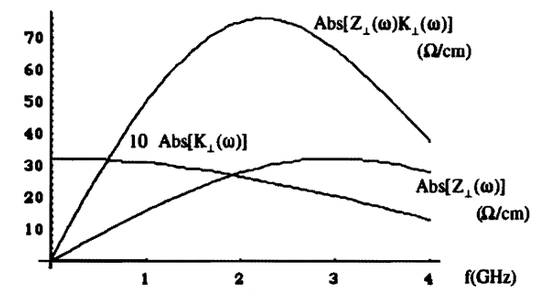

Fig. 20
Variation of pickup, kicker sensitivities, and their product, with frequency, for the Fermilab Debuncher

g_A at mid-band typically 140 dB; hence, from the figure, $\langle Z_\perp K_\perp\rangle \approx 60\ \Omega/cm$, so $\langle F\rangle \approx 10^{140/20}$x60Ω/cm = 6x10^{8}Ω/cm. Other parameters: $n_P = n_K = 128$; $\beta_{PU}=\beta_K=780$ cm; f=590 kHz; $\beta_k \approx 1$; E=8x10^9 eV; N=7x10^7 (design). Then

$$h(\text{mid-band}) = 6\text{x}10^8\Omega/\text{cm}\text{x}\frac{1.6\text{x}10^{-19}\text{x}5.9\text{x}10^5\text{x}7\text{x}10^7\text{x}780\text{x}128\ \text{cm}}{8\text{x}10^9\ \Omega} = .05$$

and

$$\frac{1}{\tau} = \frac{2x10^9}{7x10^7}x0.1 = 2.8\ Hz$$

The total damping rate will be smaller since it needs to include the heating terms also.

3. Heating from other particles (Schottky noise)

(a). Heating rate. For no Schottky band overlap, the rate of mean square emittance change resulting from to fluctuations in the pickup signals due to the finite number N of particles in the beam (Schottky noise) is

$$\left\langle\frac{[\Delta\varepsilon]^2}{\Delta t}\right\rangle = \frac{\pi N e^4 f^4 \beta_{PU}\beta_K n_P n_K \varepsilon^2}{2(\beta_k^2 E)^2}\phi(\omega_k)\sum_{\substack{n=-\infty \\ \pm}}^{\infty}|F(\{n\pm Q\}\omega)|^2\frac{1}{n\pm Q} \tag{3.37}$$

Since

$$\frac{1}{\varepsilon^2}\frac{d\varepsilon^2}{dt}=\frac{2}{\varepsilon}\frac{d\varepsilon}{dt}=-\frac{2}{\tau} \tag{3.38}$$

the incoherent contribution to the emittance damping rate for particle k, due to other particles in the beam is

$$\frac{1}{\tau_{Sch}}=-\frac{\pi N e^2 f^4 \beta_{PU}\beta_K n_P n_K}{4\left(\beta_k^2 E\right)^2}\phi(\omega)\sum_{\substack{n=-\infty\\ \pm}}^{\infty}\left|F(\{n\pm Q\}\omega)\right|^2\frac{1}{n\pm Q} \tag{3.39}$$

(b). Simplifying assumptions. Using h_n defined above in Eq. (3.31),

$$\frac{1}{\tau_{Sch}}=-\frac{\pi f^2}{2N}\phi(\omega)\sum_{n=-\infty}^{\infty}\left|h_n\right|^2\frac{1}{n+Q}=-\frac{f}{2N}\sum_{n=-\infty}^{\infty}\left|h_n\right|^2 M_n \tag{3.40}$$

where

$$M_n=\pi\frac{f\phi(\omega)}{n+Q}\approx\frac{f}{2n\Delta f} \tag{3.41}$$

is the "mixing factor" at harmonic n. The last equation follows for a rectangular longitudinal beam frequency distribution, of full width Δf_k. The mixing factor is generally >1 and approaches 1 at harmonics for which the Schottky betatron sidebands overlap: $n_{overlap}\Delta f\approx\frac{f}{2}$. Ideally, this occurs at the top end of the system bandwidth. If we take h_n as constant over the system bandwidth W, and equal to the average h defined above. in Eq. (3.36), then, converting the sum to an integral gives

$$\sum_{n=-\infty}^{\infty}M_n\approx 2\pi f\phi(\omega)\int_{f_1}^{f_2}\frac{df'}{f'}=2\pi f\phi(\omega)\ln(2) \tag{3.42}$$

so

$$\frac{1}{\tau_{Sch}}=-\frac{W}{N}\left|h\right|^2\left[\frac{\pi f^2\phi(\omega)\ln 2}{W}\right]=-\frac{W}{N}\left|h\right|^2 M \tag{3.43}$$

in which

$$M=\frac{\phi(\omega)\pi f^2\ln(2)}{W}\approx\frac{f^2\ln(2)}{2W\Delta f} \tag{3.44}$$

is the average mixing factor (as in Eq. (3.5)).

(c). Example: Fermilab Debuncher transverse cooling.[30,31]. Using h=0.05 (from 2(d).above),

$$\frac{\Delta f}{f}=\eta\frac{\Delta p}{p}=.0055\text{x}.002=1.1\text{x}10^{-5}$$

$$M=\frac{f}{\Delta f}\frac{f\ln(2)}{2W}=\frac{5.9\text{x}10^5\text{x}.7}{2\text{x}2\text{x}10^9\text{x}1.1\text{x}10^{-5}}=9.3$$

This is a rather large mixing factor. In the collection ring, the small value of η required for the bunch-manipulation RF gymnastics forces this compromise. The Schottky noise contribution to damping rate is then

$$\frac{1}{\tau_{Sch}}=-\frac{2x10^9}{7x10^7}x0.05^2x9.3=-0.65\ Hz$$

4. Heating from electronic noise

(a). Heating rate. The other incoherent contribution is due to electronic noise (primarily thermal noise in the pickup and preamplifier). This contribution is given by writing the incoherent damping rate due to Schottky noise (Eq. (3.39)):

$$\frac{1}{\tau_{Sch}}\approx-\frac{e^2 f^2\beta_K n_K R_0}{2\varepsilon\left(\beta_k^2 E\right)^2}\sum_{\substack{n=-\infty\\ \pm}}^{\infty}\left|K_\perp(\{n\pm Q\}\omega_j)g_A(\{n\pm Q\}\omega)\right|^2\frac{dP_{Sch}}{df} \tag{3.45}$$

in terms of the Schottky power density at harmonic $n\pm Q_j$:

$$\frac{dP_{Sch}}{df}=2\pi\frac{dP_{Sch}}{d((n\pm Q)\omega)}=\pi\phi(\omega)\frac{N(ef)^2}{2R_0}\varepsilon\beta_{PU}n_P\frac{\left|Z_\perp(\{n\pm Q\}\omega)\right|^2}{(n\pm Q)} \tag{3.46}$$

If the thermal noise density is designated by $\frac{dP_{thermal}}{df}$, then the emittance (anti-)damping contribution from this source has the same form as above with this power density substituted for the Schottky noise density, namely

$$\frac{1}{\tau_{thermal}}\approx-\frac{e^2 f^2\beta_K n_K R_0}{2\varepsilon\left(\beta_k^2 E\right)^2}\sum_{\substack{n=-\infty\\ \pm}}^{\infty}\left|K_\perp(\{n\pm Q\}\omega)g_A(\{n\pm Q\}\omega)\right|^2\frac{dP_{thermal}}{df}(\{n\pm Q\}f) \tag{3.47}$$

The thermal noise density is

$$\frac{dP_{thermal}}{df}=\frac{k}{2}(T_R+T_A) \tag{3.48}$$

where T_R and T_A are, respectively, the absolute temperatures of the pickup terminating resistor and the preamplifier. To reduce this contribution to the heating rate, the preamplifier and its terminating resistor are often cooled to cryogenic temperatures.

(b). Simplifying assumptions. Using again h_n defined above in Eq. (3.31), we have

$$\frac{1}{\tau_{thermal}}=-\frac{f}{2N}\sum_{n=-\infty}^{\infty}\left|h_n\right|^2 U_n \tag{3.49}$$

in which

$$U_n = \frac{2R_0}{e^2 N\beta_{PU} n_p f\varepsilon} \frac{\frac{dP_{thermal}}{df}(\{n \pm Q\}f)}{|Z_\perp(\{n+Q\}\omega)|^2}$$

$$= \frac{k(T_A + T_R)R_0}{e^2 N\beta_{PU} n_p f\varepsilon |Z_\perp(\{n+Q\}\omega)|^2} \tag{3.50}$$

U is called the "noise-to-signal" ratio:

$$U_n = \frac{\frac{dP_{thermal}}{df}}{\frac{dP_{Sch}}{df}} \frac{\pi\phi(\omega)f}{(n+Q)} = M_n \frac{\frac{dP_{thermal}}{df}}{\frac{dP_{Sch}}{df}} \tag{3.51}$$

If h_n is taken constant and equal to its average h, given above in Eq. (3.36), then

$$\frac{1}{\tau_{thermal}} = -\frac{W}{N}|h|^2 U \tag{3.52}$$

in which

$$U = \frac{\int_{f_1}^{f_2} df' U_n}{W} \tag{3.53}$$

(c). Example: Fermilab Debuncher transverse cooling. [30,31].

The parameters are n_P = 128; β_{PU}=780 cm; f=590 kHz; $\beta_k \approx 1$; E=8x10^9 eV; N=7x10^7 (design); $|Z_\perp(\omega)|$ = 30Ω / cm (mid-band); πε (initial, rms) = 3πx10^{-4} cm-rad; T_A= 40°; T_R=80°; (note cryogenic temperatures). Then

$$U_n = \frac{1.38\text{x}10^{-23}\text{x}(80+40)\text{x}50}{(1.6\text{x}10^{-19})^2 7\text{x}10^7\text{x}780\text{x}128\text{x}5.9\text{x}10^5\text{x}3\text{x}10^{-4}\text{x}30^2} = 2.8$$

h=0.05 (from above); so

$$\frac{1}{\tau_{thermal}} = -\frac{2\text{x}10^9}{7\text{x}10^7} 0.05^2\text{x}.92 = -.2 \text{ Hz}$$

5. Overall damping rate and emittance time evolution

(a). Overall damping rate. Putting all the terms together, we have

$$\frac{1}{\tau} = \frac{f}{N}\sum_{n=-\infty}^{\infty}\left(\frac{1}{\tau}\right)_n ; \left(\frac{1}{\tau}\right)_n = h_n - \frac{|h_n|^2}{2}(M_n + U_n) \tag{3.54}$$

$$h_{n,opt} = \frac{1}{M_n + U_n} ; \left(\frac{1}{\tau}\right)_{n,opt} = \frac{1}{2(M_n + U_n)} \tag{3.55}$$

In bandwidth-averaged form:

$$\frac{1}{\tau} = \frac{2W}{N}\left[h - \frac{|h|^2}{2}(M+U)\right] \tag{3.56}$$

Optimum gain:

$$h_{opt} = \frac{1}{M+U} ; \frac{1}{\tau_{opt}} = \frac{W}{N(M+U)} \tag{3.57}$$

(b).Time evolution of the emittance. From Eq. (3.56),

$$\frac{1}{\tau} = -\frac{1}{\varepsilon}\frac{d\varepsilon}{dt} = \frac{2W}{N}\left[h - \frac{|h|^2}{2}(M+U)\right] \text{but } U = U_0\frac{\varepsilon_0}{\varepsilon} \tag{3.58}$$

This equation is of the form

$$\frac{d\varepsilon}{dt} = -k_0\varepsilon + k_1, \text{ with } k_0 = \frac{2W}{N}\left[h - \frac{|h|^2}{2}M\right] \text{ and } k_1 = \frac{2W}{N}\frac{|h|^2}{2}U_0 \tag{3.59}$$

The solution is

$$\varepsilon(t) = \varepsilon_0\left\{Exp[-k_0 t] + \frac{k_1}{k_0}(1 - Exp[-k_0 t])\right\} \tag{3.60}$$

Asymptotically, the emittance is cooled to

$$\frac{\varepsilon_\infty}{\varepsilon_0} = \frac{k_1}{k_0} = \frac{U_0}{\left[\frac{2}{h} - M\right]} \tag{3.61}$$

At optimum gain

$$\left(\frac{\varepsilon_\infty}{\varepsilon_0}\right)_{opt} = \frac{U_0}{[M + 2U_0]} \tag{3.62}$$

(c). Example: Fermilab Debuncher transverse cooling [30,31].

$$h_{opt} = \frac{1}{9.3+2.8} = .08; \frac{1}{\tau_{opt}} = \frac{2\text{x}10^9}{7\text{x}10^7(9.3+2.8)} = 2.3 \text{ Hz}$$

The system is generally not operated at the optimum gain because of the large amount of microwave power required (several kilowatts). Hence the actual performance is (with h=0.05)

$$\frac{1}{\tau} = \frac{1}{\tau_{Coh}} + \frac{1}{\tau_{Schottky}} + \frac{1}{\tau_{Thermal}}$$

$$= 2.8 \text{ Hz} - 0.65 \text{ Hz} - .2 \text{ Hz} = 1.95 \text{ Hz}$$

The asymptotic emittance is

$$\frac{\varepsilon(\infty)}{\varepsilon_i} = \frac{2.8}{\left[\frac{2}{.05} - 9.3\right]} = 0.1$$

For an input emittance of 20 π mm-mrad, the beam cools asymptotically to about 2π mm-mrad.

6. *Beam feedback: coherent effects*

(a).Modification to the system gain. The kicker's coherent effect on the sample (gx_b) is fed back into the system by the beam on the next revolution, if there is insufficient sample mixing on one turn to remove the coherency. This is very similar to the gain modification which occurs in a standard feedback system: the gain with feedback g' is related to the open-loop gain g by

$$g' = \frac{g}{1+\beta g} \tag{3.63}$$

in which β depends on the feedback network (in this case, the beam transfer function). In the cooling system, the equivalent of g (h_n, at the nth harmonic) is modified as follows:

$$h_n -> \frac{h_n}{1+\frac{M_n h_n}{2}} = h_n T_n \tag{3.64}$$

in which

$$T_n = \frac{1}{1+\frac{M_n h_n}{2}} \tag{3.65}$$

depends on the beam frequency distribution through M_n; the result above is correct for a rectangular frequency distribution, for which M_n is given in Eq.(3.41) above. Then, the cooling rate nth harmonic contribution, with beam feedback included, becomes

$$\left(\frac{1}{\tau}\right)_n = h_n T_n - \frac{|h_n T_n|^2}{2}(M_n + U_n) \tag{3.66}$$

The optimum now occurs when

$$h_{n,opt} T_{n,opt} = \frac{h_{n,opt}}{1+\frac{M_n h_{n,opt}}{2}} = \frac{1}{M_n + U_n}; \; h_{n,opt} = \frac{1}{\frac{M_n}{2} + U_n} \tag{3.67}$$

For M>>U, the optimum gain is increased by a factor of 2. Note that the cooling rate at the optimum is the same as before. However, at h_{opt}, the beam transfer function gives

$$T_{n,opt} = \frac{1}{1+\frac{M_n}{M_n + 2U_n}} \rightarrow \frac{1}{2} \quad \text{if } U_n << M_n \tag{3.68}$$

At the optimum gain, neglecting the noise contribution, the cooling system provides "signal suppression" of all signals by a factor of two. This fact is sometimes used in adjusting cooling systems.

(b). Example: Fermilab Debuncher. M=9.3; U=2.8; h=0.05. Then

$$T = \frac{1}{1+\frac{Mh}{2}} = \frac{1}{1+.233} = 0.811$$

As noted above, we are not at the optimum gain, which, with feedback, corresponds to

$$h_{opt} = \frac{1}{\frac{M}{2}+U} = \frac{1}{\frac{9.3}{2}+2.8} = 0.134$$

The cooling rate, including beam feedback effects, is

$$\frac{1}{\tau} = \frac{2W}{N}\left[hT - \frac{|hT|^2}{2}(M+U)\right]$$

$$= \frac{4x10^9}{7x10^7}\left[0.05x.811 - \frac{|0.05x.811|^2}{2}(9.3+2.8)\right] = 1.75 \; Hz$$

slightly smaller than the value obtained ignoring feedback.

B. Longitudinal Stochastic Cooling

Longitudinal stochastic cooling may be used in the collection ring to further reduce the momentum spread of the debunched beam prior to transfer to the accumulation ring. This process is similar to transverse cooling--except that pickup definition of "center" is a little trickier. There are two techniques to establish a "central energy":

(1) a dipole (position-sensitive) pickup located in a region of the machine in which there is a correlation between the beam's position and its momentum ("Palmer" cooling, Fig. 21)

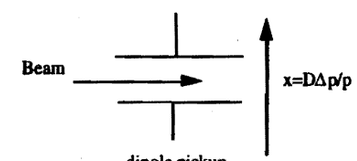

dipole pickup
Fig. 21
Palmer Cooling

The analysis is very similar to the transverse case: in simplification where we assume perfect correlation at pickup and kicker between position and momentum, we get

$$\frac{1}{\tau_{|\Delta p|^2}} = \frac{W}{N}\left[2g - g^2(M+U)\right] \tag{3.69}$$

Note: both M and U now increase as Δp/p decreases, so the cooling rate will vary in a complicated as the beam is cooled. The analysis is similar to that outlined above for transverse cooling, with this additional complication.

2) a longitudinal ("sum") pickup measures the frequency distribution of the beam; an electronic "notch" filter, which provides a frequency-dependent gain is introduced into the cooling system. The filter "notch" can be adjusted to make the gain minimize at a

frequency corresponding to the central beam revolution frequency (energy) about which we want to cool the beam. ("Thorndahl" cooling, Fig. 22)

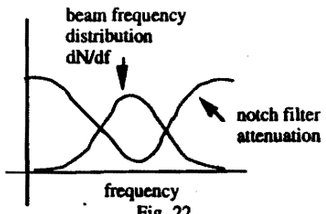

Fig. 22
Thorndahl Cooling

A detailed analysis requires a treatment along the lines discussed below for the stochastic stacking system in the accumulation ring.

C. Other issues in the collection ring [32,33]

The transverse and momentum apertures of the collection ring often set the limit on the antiproton collection rate, and so should be carefully maximized. The transverse apertures are generally limited by physical constraints, as beam dynamics does not play a very important role due to the short storage time. The design of the ring lattice, and the physical dimensions of the cooling pickups and kickers, must respect the need for maximum transverse physical aperture. The momentum aperture may be set by the maxim voltage available on the bunch rotation cavities.

IV. THE ANTIPROTON ACCUMULATION RING

The beam from the collection ring is injected into the accumulation ring, where it will be stored for many hours. The injected beam is accelerated by a conventional rf system [34] from the injection orbit into the "stack-tail" stochastic cooling system. In this system, the beam is "stochastically stacked" in longitudinal phase space (Fig. 23). Stochastic stacking[35]. is a form of longitudinal stochastic cooling. It requires a more sophisticated analysis than simply dealing with time dependence of the second moments of the distribution. The Fokker-Planck equation is used to describe the evolution of the beam distribution function.

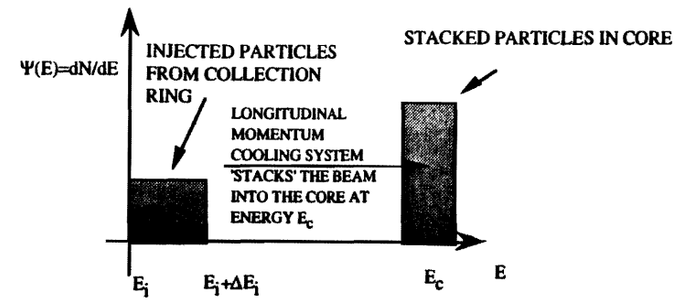

Fig. 23
Stochastic Stacking

A. The Fokker-Planck Equation

1. Particle flux equation

A longitudinal pickup (similar to the loop coupler in Fig. 18, but operated in sum mode) measures the energy of a sample ΔN of particles. The energy measurement is accomplished by one or both of the techniques mentioned above for longitudinal stochastic cooling. The signal is amplified and delivered to the kicker, which changes the sample's energy by ΔE (Fig. 24). Particles are accelerated; the density increases with energy because the process incorporates longitudinal stochastic cooling along with the acceleration ("stochastic stacking")

The flux passing E_0 due to action of a kicker delivering ΔE is estimated as follows.

ΔN = number of particles passing E_0= crosshatched area in graph

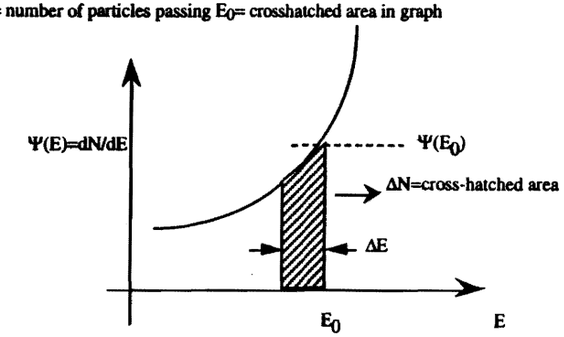

Fig. 24
Illustrating the development of the equation for the particle flux

The pickup measures the energy of a sample ΔN of particles at energy $E - \Delta E$; the kicker changes the sample's energy by ΔE. This results in a particle flux ($\Phi = dN/dt$) along the energy axis

$$\Phi = \Psi \; f\langle \Delta E\rangle_{turn} - \frac{1}{2}\frac{d\Psi}{dE} f\left\langle (\Delta E)^2 \right\rangle_{turn} \tag{4.1}$$

in which f= revolution frequency, and $\langle \Delta E\rangle_{turn}$ = average *coherent* energy gain per turn = eV(E), where V(E) is the voltage on the kicker. $\left\langle (\Delta E)^2 \right\rangle_{turn}$ = mean-square energy delivered to the beam per turn.

An explicit expression for the voltage V(E) can be given in terms of the pickup, kicker, and amplifier parameters. We refer to the loop coupler pickup in Fig. 18 above: the sum voltage is

$$V_{PU}(E,t) = ef \sum_{n=-\infty}^{\infty} Z_{\parallel}(n\omega, E) Exp[in\omega(t - t_{PU})] \tag{4.2}$$

The effective longitudinal impedance $Z_{\parallel}$ is [28]

$$Z_{\parallel}(n\omega, E) = \sqrt{\frac{R_0 Z_L}{2}} d_{\parallel}(E) Sin[\theta(\omega)] Exp[i(\frac{\pi}{2} - \theta(\omega))] \tag{4.3}$$

The transverse sensitivity $d_{\parallel}(E)$ is given an explicit energy dependence. This comes about because the pickup is often located in a dispersive region of the ring. The energy E is measured relative to that of the closed orbit point through the center of the pickup. The transverse sensitivity varies with x, the horizontal distance from the pickup centroid (see Fig. 18); in a dispersive region, $x = DE/E_0$, and

$$d_{\parallel}(E) = \frac{2}{\pi} Tan^{-1}\left(\frac{Sinh\left[\frac{\pi w}{2h}\right]}{Cosh\left[\frac{\pi DE}{2hE_0}\right]} \right) \tag{4.4}$$

in which E_0 is the beam total energy, E is the energy difference relative to that of the on-axis particle, and D is the dispersion at the pickup. Far off axis (for $\frac{\pi DE}{2hE_0} >> 1$), the sensitivity falls off like $d_{\parallel}(E) -> \frac{4}{\pi} Sinh\left[\frac{\pi w}{2h}\right] Exp\left[-\frac{\pi DE}{2hE_0}\right]$. This provides a mechanism for shaping the gain of the cooling system to an exponential energy response, which, as discussed below, will be required for the "stack-tail" cooling system.

The voltage delivered to the kicker is

$$V_K(E,t) = ef \sum_{n=-\infty}^{\infty} Z_{\parallel}(n\omega, E) Exp[in\omega(t - \frac{L}{c}) - in\omega t_{PU}] g_A(n\omega, E) \tag{4.5}$$

in which the amplifier gain $g_A(n\omega, E)$ also has an explicit energy dependence (such as might come from a notch filter). L is the system electrical length. The voltage sampled by the beam, averaged over many revolutions, is

$$V(E) = ef\sqrt{n_P n_K} \sum_{n=-\infty}^{\infty} Z_{\parallel}(n\omega, E) g_A(n\omega, E) K_{\parallel}(n\omega) Exp[-in\theta_{PK} \frac{\Delta\omega}{\bar{\omega}}] \tag{4.6}$$

for n_P pickups and n_K kickers. The kicker sensitivity (assumed to be at a zero dispersion point) is

$$K_{\parallel}(n\omega) = \frac{2Z_{\parallel}(n\omega, 0)}{R_0} \tag{4.7}$$

V(E) is the coherent voltage which produces cooling. The exponential in Eq. (4.6) expresses the "bad mixing" effect.

$\left\langle (\Delta E)^2 \right\rangle_{turn}$ is the incoherent (heating) contribution. As seen below, this will result in a diffusion term in the Fokker-Planck equation. Physically, it arises from Schottky noise, electronic noise, and other diffusive mechanisms (such as intrabeam scattering) to which the beam is subject. The Schottky contribution may be obtained by the same sort of analysis as in the transverse cooling case. The mean square energy fluctuations per unit time due to Schottky noise are

$$\left\langle \frac{[V(E)]^2}{\Delta t} \right\rangle = 2\pi N e^2 f^4 \phi(\omega) n_P n_K \sum_{n=-\infty}^{\infty} \left| Z_{\parallel}(n\omega, E) g_A(n\omega, E) K_{\parallel}(n\omega) \right|^2 \frac{1}{n} \tag{4.8}$$

Writing the beam frequency distribution in terms of the energy distribution

$$\phi(\omega) = \frac{p\beta_k \Psi(E)}{N|\eta| 2\pi f} \tag{4.9}$$

Here $|\eta| = \frac{df/f}{dp/p}$. The mean-square energy change of the beam per turn due to Schottky noise is

$$\left\langle (\Delta E)^2 \right\rangle_{turn,Sch} = \left\langle \frac{[eV(E)]^2}{\Delta t} \right\rangle T = e^4 f^2 \frac{p\beta_k \Psi(E)}{|\eta|} n_P n_K \sum_{n=-\infty}^{\infty} \left| Z_{\parallel}(n\omega, E) g_A(n\omega, E) K_{\parallel}(n\omega) \right|^2 \frac{1}{n} \tag{4.10}$$

Similarly, for the amplifier noise contributions we have

$$\begin{aligned} \left\langle (\Delta E)^2 \right\rangle_{turn,elec} &= e^2 f R_0 \frac{dP_{thermal}}{df} n_K \sum_{n=-\infty}^{\infty} \left| g_A(n\omega, E) K_{\parallel}(n\omega) \right|^2 \\ &= e^2 f R_0 \frac{k}{2}(T_R + T_A) n_K \sum_{n=-\infty}^{\infty} \left| g_A(n\omega, E) K_{\parallel}(n\omega) \right|^2 \end{aligned} \tag{4.11}$$

2 Beam feedback

As in the transverse case, the beam will form a closed loop with the cooling system, providing negative feedback into the cooling amplifier. The amplifier gain is modified as follows:

$$g_A(\omega,E) \rightarrow \frac{g_A(\omega,E)}{1+g_A(\omega,E)\beta(\omega,E)} \tag{4.12}$$

in which the feedback network analog is given in terms of an integral over the gradient of the beam's energy distribution:

$$\beta(\omega,E) = iZ_{11}(\omega,E)e^2 f^2 \sum_{n=0}^{\infty}\int dE' \frac{\partial\Psi}{\partial E'} \frac{Exp\left[in\theta_{PK}\right]}{\omega - n\overline{\omega}\left[1-\frac{E'|\eta|}{\beta_k p}\right]} \tag{4.13}$$

This expression for $g_A(\omega,E)$ should be used in the relations above to account for beam feedback. As with any feedback system, the amplifier and feedback network must be designed to provide sufficient gain and phase margin from instability.; in this case, this must be done for all frequencies within the system bandwidth, for all beam energies within the stack, and for all expected values of the beam energy density gradient. This requires careful design, performed whit the use of codes.

2. Simplify assumptions to obtain a Fokker-Planck equation

We neglect beam feedback and "bad mixing". Averaging pickup impedance, amplifier gain, and kicker sensitivity over the system bandwidth W from f_1 to f_2, we have

$$V(E) \approx 2eh(E)W$$
$$h(E) = \sqrt{n_p n_K}\left\langle Z_{11}(n\overline{\omega},E)g_A(n\overline{\omega},E)K_{11}(n\overline{\omega})\right\rangle \tag{4.14}$$

where the average is over the system bandwidth; and

$$\left\langle(\Delta E)^2\right\rangle_{noise,Sch} = 2e^4 f^2 \frac{p\beta_k\Psi(E)}{|\eta|} ln\left[\frac{f_2}{f_1}\right]|h(E)|^2 = e^2 f^2 \frac{p\beta_k\Psi(E)}{2|\eta|W^2}V(E)^2 ln\left[\frac{f_2}{f_1}\right] \tag{4.15}$$

Combining the noise contributions gives

$$\left\langle(\Delta E)^2\right\rangle_{noise} = 2\left(AV(E)^2\Psi(E) + D_N(E)\right) \tag{4.16}$$

in which

$$A = e^2 f^2 \frac{p\beta_k ln\left[\frac{f_2}{f_1}\right]}{4|\eta|W^2} \tag{4.17}$$

and

$$D_N(E) = e^2 f R_0 \frac{k}{4}(T_K + T_A)n_K \sum_{n=-\infty}^{\infty}\left|g_A(n\omega,E)K_{11}(n\omega)\right|^2 \tag{4.18}$$

The first term is due to Schottky noise, the second to system electrical noise.

Then the equation for the flux becomes

$$\Phi = feV(E)\Psi(E) - f\left(AV(E)^2\Psi(E) + D_N(E)\right)\frac{\partial\Psi}{\partial E} \tag{4.16}$$

Use of the continuity equation

$$\frac{\partial\Psi}{\partial t} + \frac{\partial\Phi}{\partial E} = 0 \tag{4.19}$$

gives

$$\frac{\partial\Psi}{\partial t} = -ef\frac{\partial}{\partial E}(V(E)\Psi(E)) + f\frac{\partial}{\partial E}\left(\left(AV(E)^2\Psi(E) + D_N(E)\right)\frac{\partial\Psi}{\partial E}\right) \tag{4.20}$$

This Fokker-Planck equation is required to describe the time evolution of the density distribution. It is generally only solved numerically, because it is nonlinear in Ψ. However, there are solutions of the static case($\frac{\partial\Psi}{\partial t} = 0$), which are instructive [35].

B. The Static "Stack-Tail" System

1. Required voltage profile

We take D_N=0 for simplicity, and n_P=n_K=1. Assume constant flux = input flux from the collector ring (Φ_0). Output flux goes into another cooling system (called the "core" system).Then the flux is

$$\Phi_0 = feV(E)\Psi(E) - f\left(AV(E)^2\Psi(E)\right)\frac{d\Psi}{dE} \tag{4.21}$$

so

$$\frac{d\Psi}{dE} = -\frac{\Phi_0}{fAV(E)^2\Psi(E)} + \frac{e}{AV(E)} \tag{4.22}$$

The pickup voltage profile V(E) is chosen to maximize $\frac{d\Psi}{dE}$:

$$\frac{d}{dV}\left(\frac{d\Psi}{dE}\right) = 0 \Rightarrow V(E) = \frac{2\Phi_0}{ef\Psi(E)}$$
$$\frac{d\Psi}{dE} = \frac{e^2 f\Psi(E)}{4A\Phi_0} \tag{4.23}$$

Solution:

$$\Psi(E) = \Psi_i exp\left(\frac{E-E_i}{E_d}\right)$$
$$E_d = \frac{4A\Phi_0}{e^2 f} = \frac{f\beta_k p\Phi_0}{|\eta|W^2} ln\left[\frac{f_2}{f_1}\right] \tag{4.24}$$

where E_i = injection energy, Ψ_i = injection density. The maximum increase in $\Psi(E)$ with energy which can be achieved is an exponential growth, with an energy scale E_d. In this case, the required voltage profile is

$$V(E) = \frac{2\Phi_0}{ef\Psi_i} exp\left(\frac{E_i - E}{E_d}\right) \tag{4.25}$$

This illustrates that the maximum increase in $\Psi(E)$ with energy which can be achieved is an exponential growth, with an energy scale E_d. In order to provide this, the voltage applied by the kicker system must decrease exponentially with the same scale factor away from the injection energy. This decrease in voltage is typically accomplished by a combination of the falloff in transverse sensitivity of dipole pickups located in dispersive regions, and the use of filters.

2. Example: Fermilab Accumulator ring stack-tail system [36]

For the Fermilab accumulator ring, the beam and machine parameters are: η = .023; f_2=2 GHz; f_1=1 GHz; W = 1 GHz; $\beta_k p$ = 8 GeV/c;Φ_0=5x10^7/sec, 1/f= 1.7x10^{-6} sec, giving

$$E_d = \frac{f\beta_k p\Phi_0}{|\eta|W^2} ln\left[\frac{f_2}{f_1}\right]$$

$$= \frac{8x10^9 x5x10^7 x0.693}{1.7x10^{-6} x.023x10^{18}} = 7 \ MeV$$

Required kicker voltage at injection: (Ψ_i=5/ev)

$$V(E_i) = \frac{2\Phi_0}{ef\Psi_i} = 34 \ volts$$

The energy scale of the whole stack is set by the required density gain:: for a density enhancement of 5x10^5, we need

$$ln\frac{\Psi(E_c)}{\Psi_i} = \frac{E_c - E_i}{E_d} = ln 5x10^5 = 13.1$$

$$E_c - E_i = 13.1 \ E_d = 92 \ MeV$$

Fig. 25 shows the stack density profile for the Fermilab accumulator.

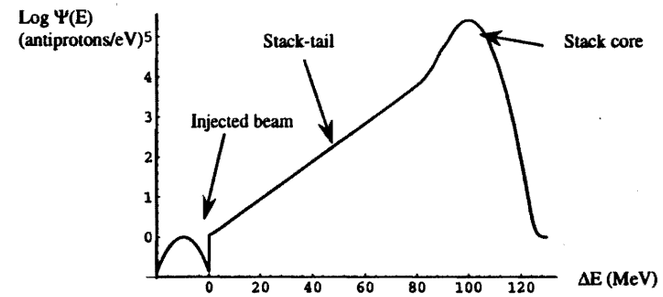

Accumulator ring
antiproton stack
Fig. 25

C. The Static "Core" System

1. Longitudinal core cooling.

The accumulator core is a longitudinal cooling system into which the flux from the stack-tail system is deposited. (See Fig. 25). In practice, one of the major limits to the operation of the stack tail system is the perturbations which it produces in the core. These may be either longitudinal or transverse (the transverse effects are caused by small misalignments in the stack trail kickers). Substantial care in pickup/kicker design and implementation is required to reduce such effects to a manageable level.

A dynamic description of the interaction between the core and the stack-tail requires numerical solution of the Fokker-Planck equation. However, a crude analysis can be made of the situation after the accumulation process using the "stack-tail" ceases. This will occur when we have reached the required total number of antiprotons (about 5x10^{11} for the original Fermilab design [37]; see Fig. 26)

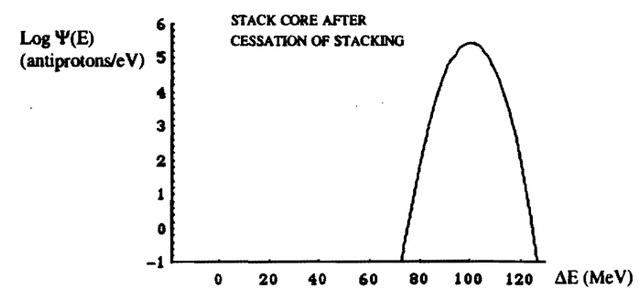

Fig. 26

Core longitudinal density distribution

In this situation, the input flux is zero and the density is stationary in time. The equation for the flux gives:

$$0 = feV\Psi - fD_N \frac{d\Psi}{dE} \tag{4.26}$$

where we have assumed that the system noise dominates over the Schottky noise, and neglected the latter. In practice, intrabeam scattering is one of the dominant contributors to the heating term D_N. The "core cooling" system (which must be physically separate from the "stack-tail" system), using one of means we have previously mentioned, establishes a voltage profile

$$V(E) = -\frac{dV}{dE}(E - E_c) \tag{4.27}$$

where E_c is the central energy of the core, and $\frac{dV}{dE}$ is a constant. Then the equation for the flux gives

$$-\frac{e}{D_N}\frac{dV}{dE}(E - E_c)dE = \frac{d\Psi}{\Psi} \tag{4.28}$$

which has as a solution

$$\Psi(E) = \Psi_0 \exp\left[-\frac{e}{2D_N}\frac{dV}{dE}(E - E_c)^2\right] \tag{4.29}$$

This corresponds to a Gaussian density distribution with an rms width

$$\sigma_e = \sqrt{\frac{D_N}{e\frac{dV}{dE}}} = \sqrt{\frac{\langle(\Delta E)^2\rangle_{noise}}{\frac{d}{dE}\langle\Delta E\rangle_{coherent}}} \tag{4.30}$$

The Fermilab system [37] has $\sigma_e = 5$ MeV.

2. Transverse core cooling.

The core also requires a transverse cooling system to reduce the transverse emittance to about 2π mm-mrad, required for the final beam to be delivered to the collider. In addition, this system is useful in controlling transverse perturbations to the core emittance caused by the stack tail system. Unlike the collection ring system, this system does not require rapid cooling.

Example-Fermilab accumulator core transverse cooling system[37]. The parameters are $\eta = .023$; $\Delta p/p = .0005$ (this is the final result of the core cooling process; T = 1.7 μsec (same as the collection ring); W = 2 GHz. Then

$$M = \frac{1}{2WT|\eta|\frac{\Delta p}{p}} = \frac{1}{2x2x10^9 x1.7x10^{-6} x.023x.0005} = 13$$

The mixing is "poor". For $N=5x10^{11}$ particles, and with a noise figure of $U_0 = .5$, the cooling rate at optimal gain is

$$\frac{1}{\tau_{\varepsilon_t}} = \frac{W}{N}\left[\frac{1}{M+U_0}\right]$$

$$= \frac{2x10^9}{5x10^{11}}\left[\frac{1}{13+.5}\right] = 3x10^{-4} \text{ Hz}$$

$$\tau_{\varepsilon_t} = 0.9 \text{ hrs}$$

An initial emittance of 7πmm-mrad from the collection ring would be reduced to 2π mm-mrad in about an hour. This is acceptable, since the accumulation time is typically more like 10-20 hours. The asymptotic emittance is

$$\varepsilon_{t\infty} = \varepsilon_{t0}\frac{U_0}{M+2U_0} = 7\frac{.5}{13+1}\pi \text{ mm-mrad}$$

$$= 0.25\pi \text{ mm-mrad}$$

D. Other issues in the accumulation ring

Although by far the dominant issues in the accumulation ring relate to stochastic cooling, there are also number of other conventional accelerator physics issues. These are generally those associated with an high quality storage ring. They include single particle and collective stability considerations; dynamic aperture and Resonances(this is a particularly difficult because the stack covers about 1.5% in momentum) ; intrabeam scattering-one incoherent process is one of the main limits to core longitudinal density. In addition, as with any stored negative ion beam, ion trapping of residual gas ions in the potential well of the negative beam can be a problem. The non-linearities associated with the ion cloud electric field can drive high-order resonances and cause emittance growth. The methods for dealing with this include the use of clearing electrodes and "beam shaking" [38].

E. Unstacking

In order to use the antiprotons in a high-energy collider, they must be efficiently extracted from the core. In the Fermilab system, a harmonic 2 rf system is used, with one of the buckets "suppressed". Beam captured in the other bucket is decelerated to the injection/extraction orbit, and kicked into a transfer line to the collider when needed [39]. (Fig. 27)

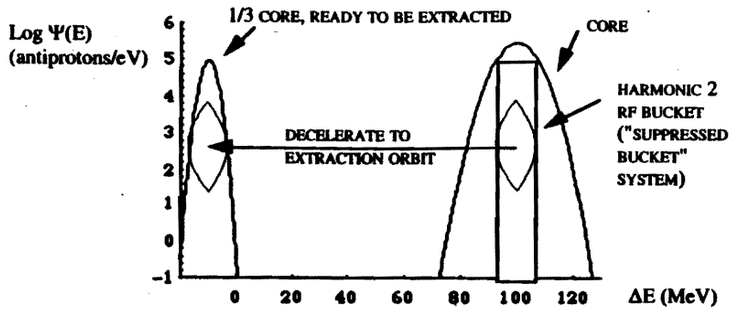

Fig. 27
Unstacking

Great care in emittance preservation during the transfer to the collider is crucial. Careful matching of all transfer lines, and sufficient aperture for close to 100% efficient transfer, is required.

V. REFERENCES

Section I
Basic Components and Major Technical Issues

[1] Design Study of a Proton-Antiproton Colliding Beam Facility, CERN/PS/AA 78-3 (1978); Design Study of an Antiproton Collector for the Antiproton Accumulator (ACOL), CERN 83-10 (1983)

[2] Design Report, Tevatron I Project, Fermilab (1984)

[3] J. Peoples, "The Fermilab Antiproton Source". IEEE Trans. on Nucl. Sci, NS-30, 1970 (1983); "Antiproton Source", in Physics of Particle Accelerators, AIP Conference Proceedings 184 (1989), p 1845

[4] M. Church, J. Marriner, "The Antiproton Sources: Design and Operation", Ann. Rev. Nucl. Part. Sci. 42,253-295 (1993)

Section II
Antiproton Production and Collection

[5] E. Jones, S. van der Meer, F. Rohner, J. C. Schnuriger, T. R. Sherwood, "Antiproton Production and Collection for the CERN Antiproton Accumulator", IEEE Trans. on Nucl. Sci., NS-30, 2778 (1983)

[6] J. V. Allaby, "Antiproton Production", in Proceedings of the CERN Accelerator School on Antiprotons for Colliding Beam Facilities, Geneva (CERN 84-15), (1984) p. 63

[7] E. Jones, "Pbar Production and Collection", in Proceedings of the CERN Accelerator School on Antiprotons for Colliding Beam Facilities, Geneva (CERN 84-15), (1984) p. 79

[8] G. Dugan, "Pbar Production and Collection at the FNAL Antiproton Source", in Proceedings of the XIII International Conference on High Energy Accelerators, p 264, Novosibirisk (1985)

[9] E. J. N. Wilson, "Antiproton Production and Accumulation", in Physics of Particle Accelerators, AIP Conference Proceedings 153 (1987), p 1650

[10] C. Hojvat, A. J. vanGinneken, "Calculations of Antiproton Yields for the Fermilab Antiproton Source", Nuclear Instruments and Methods 206, 67 (1983)

[11] I.L. Azhgirey, N. V. Mokhov, S. I. Striganov, "Antiproton Production for Tevatron", Fermilab internal report (1990)

[12] S. C. O'Day, F. M. Bienosek, "8.9 GeV Antiproton Yield Measurements at the Fermilab Antiproton Source", Nuclear Instruments and Methods A343, 343 (1994)

[13] Proceedings of the High Intensity Targeting Workshop, Fermilab (April 28-30, 1980)

[14] S. O'Day, F. Bienosek, K. Anderson, "New Target results from the FNAL Antiproton Source", in Proceedings of the 1993 Particle Accelerator Conference, p 3096 (1994)

[15] F. M. Bienosek, K.Anderson, K. Fullett, "Requirements for a Beam Sweeping System for the Fermilab Antiproton Source Target", in Proceedings of the 1995 Particle Accelerator Conference, p 1939 (1996)

[16] J. Griffin, J. MacLachlan, A. G. Ruggiero, K. Takayama, "Time and Momentum Exchange for Production and Collection of Intense Antiproton Beams at Fermilab", IEEE Trans. on Nucl. Sci., NS-30, 2630 (1983)

Section III
The Antiproton Collection Ring

[17] S. van der Meer, "Stochastic Damping of Betatron Oscillations in the ISR", CERN/ISR/PO/72-31

[18] F. Sacherer, "Stochastic Cooling Theory", CERN/ISR/TH/78-11

[19] D. Mohl, G. Petrucci, L. Thorndahl, S. van der Meer, "Physics and Technique of Stochastic Cooling", Phys. Rept. 58, 2 (1980) 73-119

[20] J. Bisogano, C. Leeman, "Stochastic Cooling", in Physics of High Energy Particle Accelerators, AIP Conference Proceedings 87 (1982), p 583

[21] A. V. Tollestrup, G. Dugan, "Elementary Stochastic Cooling", in Physics of High Energy Particle Accelerators, AIP Conference Proceedings 105 (1983), p 954

[22] D. Mohl, "Stochastic Cooling for Beginners", in Proceedings of the CERN Accelerator School on Antiprotons for Colliding Beam Facilities, Geneva (CERN 84-15), (1984) p. 97

[23] S. van der Meer, "Optimum Gain and Phase for Stochastic Cooling Systems", in Proceedings of the CERN Accelerator School on Antiprotons for Colliding Beam Facilities, Geneva (CERN 84-15), (1984) p. 183

[24] D. Mohl, "Stochastic Cooling", in Proceedings of the CERN Accelerator School on Advanced Accelerator Physics, Oxford (CERN 87-03), (1987) p. 453

[25] S. van der Meer, "An Introduction to Stochastic Cooling", in Physics of Particle Accelerators, AIP Conference Proceedings 153 (1987), p 1618

[26] J. Marriner, "Review of the Physics, and Practice of Stochastic Beam Cooling", Proceedings of the 1987 Particle Accelerator Conference, p. 1383 (1987)

[27]B. Autin, G Carron, F. Caspers, S. Milner, L. Thorndahl, S. van der Meer, "ACOL Stochastic Cooling Systems", Proceedings of the 1987 Particle Accelerator Conference, p. 1549 (1987)

[28] G. Lambertson, "Dynamic Devices-Pickups and Kickers", in Physics of Particle Accelerators, AIP Conference Proceedings 153 (1987), p 1413

[29] C. S. Taylor, "Stochastic Cooling Hardware", in Proceedings of the CERN Accelerator School on Antiprotons for Colliding Beam Facilities, Geneva (CERN 84-15), (1984) p. 181

[30] B. Autin, J. Marriner, A. G. Ruggiero, K. Takayama, "Fast Betatron Cooling in the Debuncher Ring in the Fermilab Tevatron", IEEE Trans. on Nucl. Sci., NS-30, 2593(1983)

[31] D. Peterson, W. Kells, J. Marriner, G. Mayer, S. Mtingwa, R. Pasquinelli, "Measurement and Performance of the Fermilab Antiproton Source Debuncher Betatron Stochastic Cooling System", Proceedings of the 1987 Particle Accelerator Conference, p. 1728 (1987)

[32] B. Autin et al, "The CERN Antiproton Collector Ring", Proceedings of the European Particle Accelerator Conference, Rome (1988), p 308

[33] B. Autin, "Lattices for antiproton rings", in Proceedings of the CERN Accelerator School on Antiprotons for Colliding Beam Facilities, Geneva (CERN 84-15), (1984) p. 33

Section IV
The Antiproton Accumulation Ring

[34] A. Ando, K. Takayama, "Effects of rf Stacking on Cooling Tail in the Fermilab Accumulator", IEEE Trans. on Nucl. Sci., NS-30, 2601(1983)

[35] S. van der Meer, "Stochastic Stacking in the Antiproton Accumulator", CERN/PS/AA/78-22 (1978)

[36] R. J. Pasquinelli, W, Hyslop, W, Kells, M. Kuchnir, J. Marriner, G. Mayer, J. McCarthy, S. Mtingwa, D. Peterson, R. Shafer, "Stacktail Momentum Cooling in the Fermilab Antiproton Source", Proceedings of the 1987 Particle Accelerator Conference, p. 1090 (1987)

[37] W. Kells, J. Marriner, R. Pasquinelli, S. Mtingwa, "Performance of Tevatron I Core Stochastic Cooling Systems", Proceedings of the 1987 Particle Accelerator Conference, p. 1090 (1987)

[38] J. Marriner, D. Mohl, Y. Orlov, A. Poncet, S. van der Meer, "Experiments and Practice in Beam Shaking", Particle Accelerators 1990, Vol. 30, p 13

[39] V. K. Bharadwaj, J. E. Griffin, D. J. Harding, J. A. Maclachlan, "Beam Transfer from the Core of the Accumulator to the Main Ring in the Fermilab Source", Proceedings of the 1987 Particle Accelerator Conference, p. 1022 (1987)